Modelling the Impacts of Crop Rotation on Soil Structure, Soil Carbon Turnover and Storage

Continued testing of a novel dual-pore system model against data collected from a long-term study site in Offer, Sweden

Mikael Dooha

Master's Degree project • 30 ECTS
Swedish University of Agricultural Sciences, SLU
Katharina Meurer and Nicholas Jarvis/Soil and Environment
Soil, Water and Environment/Master of Science
Examensarbeten, Institutionen för mark och miljö, SLU, 2020:12
Uppsala 2020

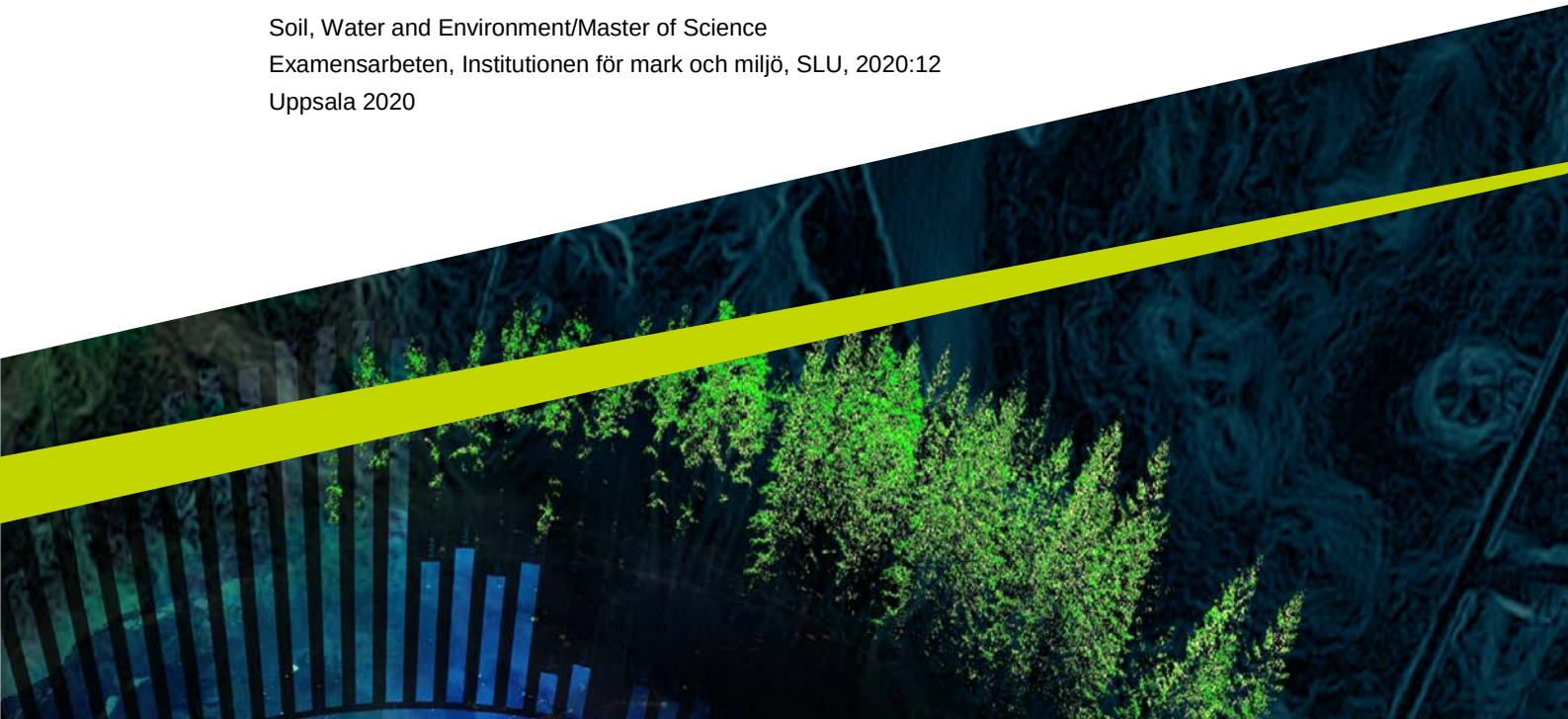

Modelling the Impacts of Crop Rotation on Soil Structure, Soil Carbon Turnover and Storage – Continued Testing of a Novel Dual-Pore Model Against Date Collected from a Long-Term Study Site in Offer, Sweden.

Mikael Dooha

Supervisor:	**Katharina Meurer, SLU, Department of Soil and Environment**
Assistant supervisor:	Nicholas Jarvis, SLU, Department of Soil and Environment
Examiner:	Thomas Keller, SLU, Department of Soil and Environment

Credits:	30 ECTS
Level:	Second cycle, A2E
Course title:	Master thesis in Soil Science, A2E
Course code:	EX0880
Programme/education:	Soil, Water and Environment - Master's Program
Course coordinating dept:	Department of Soil and Environment
Place of publication:	Uppsala
Year of publication:	2020
Title of series:	Examensarbeten, Institutionen för mark och miljö, SLU
Part number:	2020:12
Keywords:	Carbon sequestration, crop rotation, humification, land-use, modelling, porosity, soil organic matter, soil structure, tillage

Swedish University of Agricultural Sciences
Faculty of Natural Resources and Agricultural Sciences
Department of Soil and Environment

Publishing and archiving

Approved students' theses at SLU are published electronically. As a student, you have the copyright to your own work and need to approve the electronic publishing. If you check the box for **YES**, the full text (pdf file) and metadata will be visible and searchable online. If you check the box for **NO**, only the metadata and the abstract will be visible and searchable online. Nevertheless, when the document is uploaded it will still be archived as a digital file.

If you are more than one author you all need to agree on a decision. Read about SLU's publishing agreement here: https://www.slu.se/en/subweb/library/publish-and-analyse/register-and-publish/agreement-for-publishing/.

☒ YES, I/we hereby give permission to publish the present thesis in accordance with the SLU agreement regarding the transfer of the right to publish a work.

☐ NO, I/we do not give permission to publish the present work. The work will still be archived and its metadata and abstract will be visible and searchable.

Abstract

As we look for solutions to the worsening climate crisis, carbon sequestration has become a popular strategy to mitigate CO_2 emissions. Carbon models are used to predict or emulate changes in future soil organic carbon (SOC) stocks, but most fail to account for the influence of pore size and soil structure on SOC storage. This study examines a new dual-pore system model with data from a long-term study site in Offer, Sweden, to determine if it is possible to predict SOC storage capacity based upon soil organic matter (SOM) retention and quality, by accounting for pore size and distribution. Data from the long-term study site provided soil samples from two different cropping treatments (A and D); yearly records of crop yield measurements; some SOC and bulk density (BD) measurements; and water content and pressure head data for 1956 and 2019.

The model simulates an increase in SOM for a prolonged ley treatment (A) and a decrease in an annual cropping treatment with tillage (D). There is a 12 percent gain of SOM in treatment A and a 32 percent loss of SOM in treatment D, attributed primarily to fluctuations in storage of microbially-processed SOM. While the model does not precisely fit the data, there is a clear correlation between the simulated and modelled SOC values - r values of 0.91 and 0.83, root mean square error (RMSE) and mean absolute error (MAE) values below 0.002, and Nash-Sutcliffe model efficiency (NSE) values of 0.71 and 0.55 for treatments A and D, respectively. For BD, the model does not fit the data for treatment A very well; but, for treatment D, a positive NSE value of 0.06 and r value of 0.66 suggests that there was some correlation. There is a near perfect fit for treatment D when the final BD measurement is removed. When accounting only for SOC and BD and assigning them equal weights, the EF values were 0.21 for treatment A and 0.31 for treatment D, indicating that the dual-pore model is relatively successful overall. A lack of data points made it difficult to evaluate overall model performance. Despite this, trends in SOC were matched reasonably well by the model. The most important finding of the study is that the model successfully calibrates an organic matter retention coefficient for treatment A (0.29) that is twice for as large as treatment D (0.15), reflecting higher organic matter quality and the developed soil structure of a prolonged grass ley. This is a promising outcome in a second test of a novel dual-pore system, dual-carbon store model.

Keywords: Carbon sequestration, crop rotation, humification, land-use, modelling, porosity, soil organic matter, soil structure, tillage

Popular Science Summary

As the effects of global warming are increasingly realized through changing climate patterns around the world, measures to reduce and remove carbon from the atmosphere have gained popularity among scientists, politicians and the media alike. "Carbon neutral" has become a marketing angle for an aviation industry that promises to offset emissions by planting trees, while carbon sequestration is touted as the single most important mitigation tactic available. However, despite decades of scientific research in the fields of soil and crop sciences and land management, the reality is that we still do not fully understand the global carbon cycle.

It is difficult to ascertain the efficacy of carbon storage as a solution to atmospheric warming, primarily due to a lack of long-term studies that examine how different crop rotations and land management techniques affect carbon flux in soils. Furthermore, even when data is available from long-term studies, it can be difficult to extrapolate due to the sheer complexity of soil processes, as well as the degrees of variation in climate and soil types around the world. An additional complication is that carbon buildup in soils is generally a slow process, so even decades-long studies might only provide a limited perspective on carbon flux and the global carbon cycle.

The best solution to overcoming this lack of knowledge we contend with is to use modelling software to predict future changes in soil carbon stocks. Carbon storage models can range in complexity and degree of sophistication; some rely on relatively simple mathematical problems run through Excel, while others are constructed from physical formulas and time series analyses that require heavy computing power. Based upon the input data used – such as temperature, water retention, or soil organic matter – these models can infer whether and to what extent carbon sequestration may be viable.

One novel factor that has not yet been studied or modelled extensively is how pore sizes in soil interact with carbon to affect degradation rates and storage capacity. Soil is generally classified according to mineral particle sizes, but soil particles aggregate at both the macro and micro-level, creating different-sized pockets – pores – through which air and liquid flow, and where carbon and other organic matter can be stored. Pore size of soil is therefore more dynamic than mineral particle size, and therefore may be a better signifier of soil carbon storage capacity.

This study uses a dual pore model to examine whether it is possible to predict the capacity for organic carbon storage in soil. Input data for the model comes from a site in Northern Sweden, where specific contrasting crop rotations have been carefully managed since 1956, varying in the length of a grass ley period. By calibrating and testing the model against the existing soil structure and carbon data from the site, the results of this study indicate that together with the quality of the SOM inputs, pore size is an important factor in soil organic carbon storage. The model was able to match the long-term trends in SOM observed in two contrasting crop rotations with reasonable accuracy.

Table of contents

List of tables

List of figures

Abbreviations

AGB	Above-Ground Biomass
AR5	IPCC Fifth Assessment Report
BD	Bulk Density
BGB	Below-Ground Biomass
GHG	Greenhouse Gas
GMST	Global Mean Surface Temperature
ICBM	Introductory Carbon Balance Model
IPCC	UN Intergovernmental Panel on Climate Change
IPCC	UN Intergovernmental Panel on Climate Change
MAC	Macropores
MAT	Matrix
MES	Mesopores
MIC	Micropores
NSE	Nash-Sutcliffe Model Efficiency
RCP	Representative Concentration Pathway
RMSE	Root Mean Squared Error
SLU	Swedish University of Agricultural Sciences
SOC	Soil Organic Carbon
SOM	Soil Organic Matter
SSE	Sum of Squared Errors
SWRC	Soil Water Retention Curve
VG	Van Genuchten (Equation)

1. Introduction

In 2014, the UN Intergovernmental Panel on Climate Change (IPCC) released its Fifth Assessment Report (AR5), the most recent comprehensive assessment regarding the current state of the climate and climate science. In AR5, the IPCC found that over the short span of 260 years - between 1750 and 2011 - atmospheric concentrations of CO_2 had increased 40% while CH_4 had increased by 150% (IPCC, 2014). Per the report, this marked the highest levels reached in 800,000 years for these greenhouse gases (GHG) (IPCC, 2014). Of this total increase in CO_2 levels, approximately half had entered the atmosphere in just the previous four decades; the period between 2000 and 2010 saw larger absolute increases than any other decade (IPCC, 2014). Furthermore, the influx of CO_2 into the atmosphere by anthropogenic emissions was a primary driver of global warming (IPCC, 2014).

As scientists, activists, and policymakers worldwide scramble for solutions to stave off the impending climate crisis, carbon sequestration has become a popular theoretical solution. A mitigation technique that involves trapping atmospheric carbon in biological or terrestrial systems, carbon sequestration as a term can refer to both natural and anthropogenic activities. The 2019 IPCC "Special Report: Climate Change and Land" outlines the efficacy of many such activities in combatting the multifarious challenges that climate change poses, including land-use practices that promote the capture and storage of atmospheric carbon in soils while decreasing the release of carbon (IPCC, 2019). Specifically, the special report lists soil organic carbon (SOC) management as one of the response options that has the capacity to address the most pertinent land-related challenges (IPCC, 2019).

1.1. Soil and the global carbon cycle

SOC accounts for a significant amount of the world's reserves, which according to Lal (2004) is as much as 3.3 times the carbon in the atmosphere and 4.5 times that in the biosphere. Tifafi *et al.* (2018) estimated these organic carbon reserves are somewhere between 2500 Pg to 3400 Pg (1 Pg = 10^{15} grams), a difference attributed to uncertainty in estimates of bulk density (BD) and boreal SOC storage. Variation in estimates of organic carbon reserves may also be compounded by the lack of a

single, consistent approach to the sampling and monitoring of soils. To account for these variations as well as a general lack of sufficient long-term data reflecting carbon dynamics in soil, models can be used to assess the cycle of SOC and predict the efficacy of carbon sequestration tactics.

In these assessments of SOC, one of the most important yet understudied factors that impacts SOC management is soil structure. The simplest definition of soil structure, offered by Oades (1993), is the "arrangement of particles and pores"; and though accurate in its simplicity, this definition understates the complexity and dynamism of soil structure formation. All soils are comprised of mineral particles, soil organic matter (SOM), water and air, but the particle and pore structure that makes up the soil profile varies depending on a number of factors: soil particle interactions, roots, macrofauna and microbial communities, chemical processes, and external factors such as climate and tillage (Oades, 1993). Soil structure therefore regulates the movement and accessibility of SOM to microorganisms, nutrients, water, and air in a soil, which in turn influences the presence of and ability for plants and micro- and macro-fauna to thrive there. Interactions between these organisms and the soil then further reshapes soil structure.

The result is that soil structure is always in flux, as these factors create a feedback system of structural formation wherein aggregate and pore formation in soil can induce processes that yield new aggregates and pores. Given that soils account for much of the global carbon stock, fluctuations in soil structure can have an outsized effect on the global carbon cycle (Schimel *et al.*, 1994). For this reason, land management practices are of utmost importance to the management of SOC, as disruptions to the soil structure due to intensive cultivation practices can lead to the release of atmospheric CO_2 rather than SOC storage. Therefore, by improving SOC models to accurately account for soil structure and carbon dynamics, it will be possible to better understand the relationship between SOC storage and land management practices, and how these can be effective tools in the fight against the climate crisis.

1.2. Aim of the thesis

This thesis examines if, by accounting for pore size distribution, it is possible to make predictions for SOC storage capacity in soil based upon the portion of organic matter easily accessible to degradation. This study utilizes an Introductory Carbon Balance Model (ICBM) that was initially developed to account for turnover of two classes of organic matter in soil, and which has since been adapted to account for hydraulic soil properties and pore size distribution. The model was previously calibrated against data from a long term study conducted in Ultuna, Sweden. In that

experiment, the model was successful in emulating SOC storage and flux, bulk density (BD), and micro-porosity in manured and bare fallow plots.

Here, the efficacy of the newly introduced dual pore model is further examined using data from a long-term study in Offer, Sweden. The experiment at Offer started in 1956; the site contains four separate crop rotations that follow a six-year cycle. Previous studies of the site have shown that crop rotations that allowed for reduced tillage yielded better soil structure and greater amounts of SOC than those that necessitate frequent tillage of the soil. Yearly records of crop yield measurements and inputs were kept, and SOC and BD was measured occasionally during the course of the study. Water retention measurements are available for 1956 and soil samples were also collected in 2019 to produce a new soil water retention curve. Given the new data of the long-term study-site, the aim of this thesis is to test whether the dual-pore model can accurately predict SOC storage capacity.

2. Background

2.1. Soil structure

Soil structure is affected by the quality and quantity of SOM present in soil, and is integral to the ability of soil to carry out ecological functions such as water filtration and storage, air filtration and storage, nutrient recycling, and carbon storage (Oades, 1993). While soils are usually classified as a combination of primary particles—sand, silt, and clay—the specific structure of a soil is defined by both particles and pores, each of various sizes, which are affected by many factors. Soil composition and human influence (i.e., tillage) can significantly impact soils, but plants, microorganisms, macrofauna and physical processes such as water flow and freeze-thaw are also key to determining soil structure, and thus, soil functions like carbon storage (Oades, 1993). Soils with high amounts of SOM therefore have a more developed structure that promotes biological productivity, increases hydraulic conductivity and air flow, and facilitates increased storage of SOM (Dexter, 1988).

Within soil, there are two types of pores: textural, and structural (Childs, 1969). Textural pores are created due to variation in the sizes and shapes of soil mineral particles and the sizes of these pores is fairly consistent within a soil type (Nimmo, 2013). Formed in the spaces between mineral particles, these pores are inherent to soil structure (Bruand & Cousin, 1995). While textural pores allow for some amounts of water and air flow through the soil, it is the formation of soil aggregates and structural pores that leads to a larger degree of movement and storage of water, air, and organic matter throughout the soil profile (Nimmo, 2013).

Soil aggregates form as a result of biological, chemical, and physical processes that in turn create structural pores (Childs, 1969). The amount and quality of SOM in soil can determine the formation of aggregates and pores through the degradation of organic matter by microbiota (Jackson *et al.*, 2017). Additionally, the filtering and storage of water and air through soil also impacts aggregation and pore formation through the physical processes of swell/shrink and freeze-thaw (Oades, 1993). Size and distribution of soil aggregates and structural pores are principal factors in the capacity of soil to store SOC, as it is through these pores that carbon,

air and water travel and therefore it is within them that degradation and storage of SOM occurs (Nimmo, 2013). Soil aggregates of varying sizes will yield different sized structural pores; classifications of aggregates and pores sizes are often not defined according to specific values but rather are best understood as a certain range within a larger spectrum, as seen in Figure 2-1(a) (Dexter, 1988).

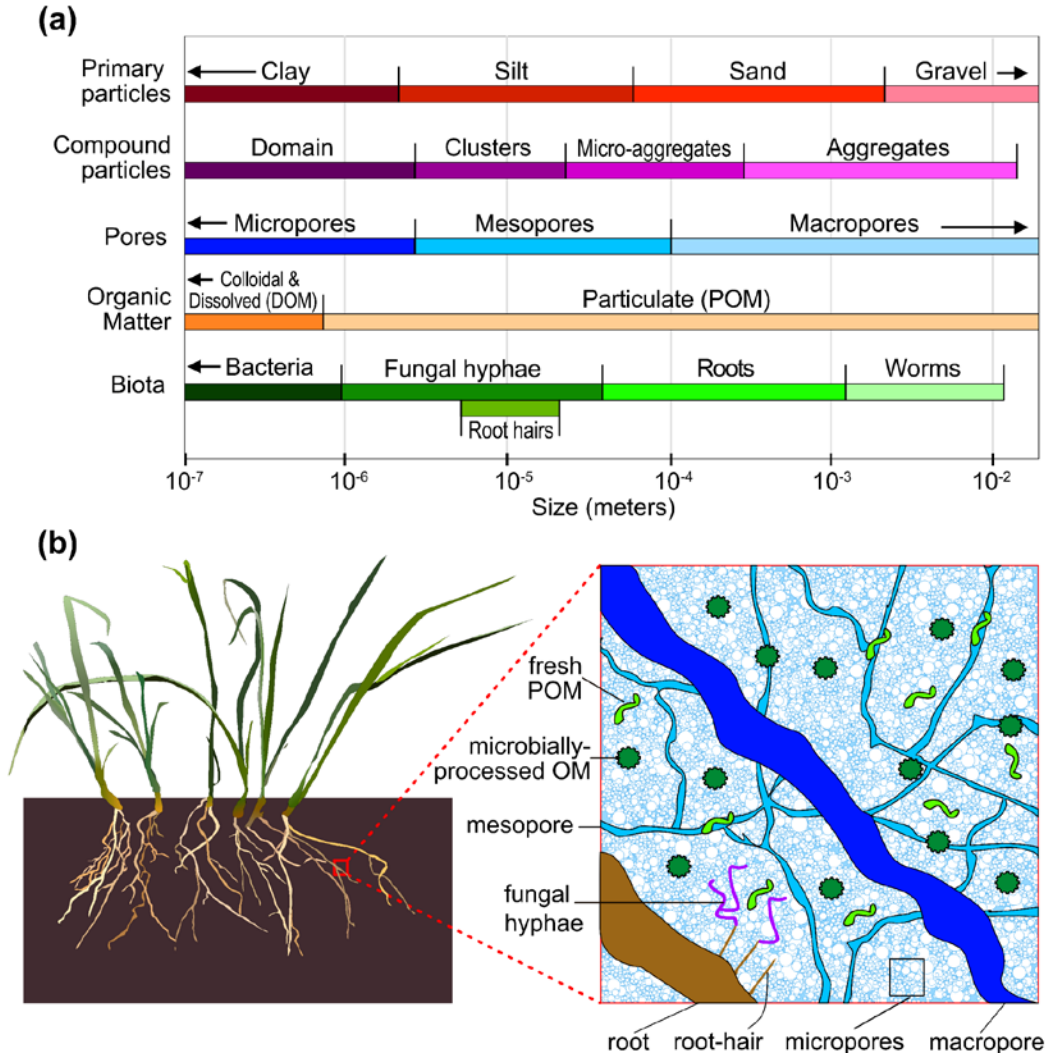

*Figure 2-1. (a) Relative size of soils particles, soil aggregates, pores, organic matter, and biota *modified figure from Dexter (1988) to include organic matter particle sizes according to Verdugo (2012). (b) Schematic of a soil profile showing the relationship between fresh particulate organic matter and microbially-processed organic matter with respect to pore structure, which influences how accessible organic matter is to forces involved in SOM degradation *modified figure from Meurer et al. (2020b).*

Pores are also often classified in three size classes: macro, meso, and micro (Dexter, 1988). Macropores are the largest pores; formed via swell/shrink and freeze-thaw processes, macrofauna activity, and root growth, these pores provide routes for preferential flow and infiltration in soils (Jarvis *et al.*, 2009; Beven & Germann, 1982). Mesopores are mid-size pores that develop primarily between aggregates due to root growth, and fungal and microbial activity (Lepore *et al.*, 2009).

Mesopores, particularly those that are interconnected, are effective in both facilitating the movement of SOC through soil as well as acting as storage for SOC (Six *et al.*, 2004). In this study, textural pores are classified as meso- or micropores, and combined as matrix pores. Micropores are the smallest pores, formed through aggregation due to microbial and fungal activity (Six *et al.*, 2004). Micropores have low levels of connectivity and tortuosity due to their size and thus are key to trapping SOC in soil (Zhou *et al.*, 2020; Nimmo, 2013). A schematic illustration of a soil profile is shown in Figure 2-1(b) to demonstrate the relationship with pore size and SOM. The pore size and distribution within a soil profile can often be determined by examining soil hydraulic properties, including tortuosity, connectivity, and soil water retention curves (SWRC) (Rawls & Pachepsky, 2002).

2.2. SOM and SOC

SOM is comprised of plant, animal, and microbial debris, all of which may be found in both living forms and varying stages of decomposition. Soil composition and health is determined by the presence of SOM, as SOM affects soil structure and porosity as well as the presence of and potential for biological activity and plant growth (FAO 2005). SOM can be classified in two primary pools: labile SOM, a smaller pool which is predominantly fresh particulate matter; and humus, a larger pool that is the more stable fraction (Cole *et al.*, 1993). An overview is presented in Table 2-1. The classification of SOM into these pools is based upon the decomposition rate of the organic material composition; thus, these pools are not constant or fixed but rather represent the movement of SOM through degrees of decay. Fluctuations in these pools are determined by climate, carbon inputs, and edaphic conditions (FAO 2005).

The labile SOM fraction is generally comprised of small particulate organic matter, which mineralizes rapidly due to high biological activity; it includes relatively fresh materials such as plant residues, microbial biomass, polysaccharides, dead organisms, and fecal material (Cole *et al.*, 1993; Hsieh, 1992). The fresh material contains a significant amount of low molecular weight aromatic acids, carbohydrates, amino acids, and other easily digestible compounds (Schnitzer, 1991). Due to the high turnover rate, labile SOM has a decomposition rate of days to years (Cole *et al.*, 1993; Hsieh, 1992).

SOM in the humus fraction is comprised of microbially decomposed carbon and takes decades to centuries to decompose; this occurs through the process of humification, in which labile SOM is transformed into carbon through the dissipation of protein and carbohydrate rich materials (Schnitzer & Monreal, 2011). Compounds in the humus fraction consist of heterogenous compounds which may

bind to mineral particles, bind to and thus deactivate enzymes, or may contain difficult to decompose substances such as lignin, oxalates, tannins, and suberin structures (Lucas *et al.*, 2018; Rasse *et al.*, 2005).

Finally, a portion of SOM may take as long as millennia to decompose and therefore is often referred to as recalcitrant SOM; however, it is likely that under the right conditions, this SOM can also be decomposed. With the exception of charcoal, structural differences are not responsible for recalcitrance, but rather the specific microbial communities, environmental conditions, enzyme activity, and a lack of accessibility of the microbes to SOM protected in small soil matrix pores can affect the susceptibility of this SOM to decomposition (Kleber, 2010).

Table 2-1. Description of SOM pools.

Pool Type	Composition	Decomposition rate
Labile	Fresh crop residues including roots and crop residues (leaves, stems, cobbs) and small particulate organic matter	days to decades
Humus	Microbially decomposed SOM (which in some cases is attached to mineral matter)	decades to centuries

Though SOM and SOC are closely related, the terms should not be used interchangeably; SOC refers explicitly to organic carbon in soil, while SOM is used to describe all organic materials in soil, including that which is not or not yet SOC. It is important to clarify this distinction as SOM and SOC are treated as separate factors in the model used in this thesis. It is estimated that SOM contains 50% C (Pribyl, 2010).

2.3. The role of land management in SOC storage

Land management practices play an important role in both present and future SOC stocks. Current SOC stocks are largely determined by a combination of land use and climatic conditions (Jarvis *et al.*, 2017), with studies indicating that cooler and more humid regions have higher SOC storage (Lal & Follett, 2009). However, if GSMT continues to rise as is expected, SOC management and agricultural practices in particular will become increasingly important to the sequestration of carbon (IPCC, 2019).

It has long been recognized that intensive farming and poor land management techniques actively contribute to the degradation of soil structure and SOM loss (Watson *et al.*, 2002). A recent study by Sanderman *et al.* (2017) estimated the

amount of carbon loss to be as great as 25 percent to 75 percent of antecedent stocks in agricultural soils under intense cultivation, which in Europe alone describes more than half of the cultivated land (Van-Camp. L. *et al.*, 2004). Declines in SOC are significant in soils that have been converted from grassland or long-term rotations of forage crops to rotations of annual crops (Bolinder *et al.*, 2010; Cole *et al.*, 1993), with data from long-term studies in Canada and northern Europe showing that the greatest loss of SOC occurs within the first decade of intensified cultivation (Kätterer & Andrén, 1999). This is largely the result of SOM loss and disruptions to soil structure that occur during the arable phase of cropping due to conventional tillage practices and annual crops (Or *et al.*, 2000; Tisdall & Oades, 1982).

Conversely, these same long-term studies demonstrate the efficacy of utilizing permanent grasslands and grass ley rotations within a cropping system to improve soil structure and SOM storage (Watson *et al.*, 2002; Kätterer & Andrén, 1999). Zhou *et al.* (2017) estimate that grasslands contain between 10 percent and 30 percent of global SOC, sequestering carbon at a rate of 0.5 Pg C $year^{-1}$. The efficacy of permanent grasslands and grass ley rotations in sequestering carbon is due to the reduction in tillage for this type of land use, increased below-ground (root) carbon inputs and the physical protection from erosion that grass leys provide (Baker *et al.*, 2007; Paustian *et al.*, 1997a). By incorporating prolonged periods of ley into a cropping system, SOM is able to accumulate during the ley phase, which leads to improved soil structure and healthier soils (Jarvis *et al.*, 2017; Watson *et al.*, 2002).

2.3.1. Macrofauna and root growth in healthy soils

Healthy soils are more likely to support vegetation and larger populations of soil macrofauna, such as earthworms; soils that have had periods of ley are particularly habitable for earthworms, as there will have been fewer tillage events (Jarvis *et al.*, 2017; Schmidt *et al.*, 2003). Considered ‘soil engineers’, both plants – due to root growth - and these macrofauna influence soil structure formation through the process of bioturbation, which results in the creation of aggregates and biopores (Jarvis *et al.*, 2017; Jones *et al.*, 1997).

The growth of plant roots causes displacement of surrounding soil particles, yielding new aggregates and pores due to the compression of the soil (Keyes *et al.*, 2016); the extent to which root growth affects soil structure will depend on the specific plant, as root types vary (Watson *et al.*, 2002). The movement of earthworms through soil has a similar displacement effect; however, earthworms additionally ingest and defect soil particles, and the resulting casts also produce new aggregates (Binet & Curmi, 1992; Dexter, 1988). The ingestion of soil by earthworms also serves to provide physical protection for SOM through the mixing that occurs during digestion (Martin, 1991).

2.4. Modelling soil organic carbon

Due to the complexity of soil structure and SOM dynamics, as well as a high degree of uncertainty regarding the effects of climate change on soil conditions, numerous models have been created to simulate aspects of SOM processes in order to assess how effective carbon sequestration may be as a climate change mitigation tactic (IPCC, 2019). SOM models generally belong to one of two categories; as described by Jandl et al. (2014), the first category of models utilizes simple equations to examine large scale carbon fluxes, while the second category of models are more complex, being designed for applications at a much smaller scale (i.e. farm plots) and examine the movement of SOM through different pools (Paustian et al., 1997b). However, since changes in SOM and soil structure occur slowly, it is necessary to couple the information provided by these models with that collected through the monitoring of long-term field studies (Jandl et al., 2014). For this reason, long-term studies such as the one conducted in Offer, Sweden are valuable sources of data on soil carbon storage against which SOM models can be calibrated and refined.

The majority of SOM models designed to study agricultural systems account for climate and soil conditions, and crop and soil properties (Bolinder *et al.*, 2012). One factor that has not been widely accounted for in SOM models is the effect of soil structure and porosity on carbon turnover. Several dual-permeability models exist which account for structural and matrix (textural) porosity to examine water flow and solute transport. A soil carbon model that accounts for the effects of pore space structure would have the advantage of accounting for dynamic hydraulic functions in combination with carbon storage (Meurer *et al.*, 2020b). A dual-pore/dual-carbon model would be able to account for the slower rate of mineralization of C in micropore regions of the soil due to the limited accessibility of microorganisms to these pores (Meurer *et al.*, 2020b).

Andrén and Kätterer (1997) created the simple Introductory Carbon Balance Model (ICBM) for simulating carbon balances at the soil profile scale, with the intention that it could be widely implemented. This model was adapted by Meurer *et al.* (2020b) to account for dual-pore systems. This is the model utilized in this study.

3. Methods

3.1. Site description

The data used to calibrate the model comes from a long-term crop rotation experiment in Offer, Sweden. The Offer study site lies just below the arctic circle (63.141457°N, 17.751473°E) at an altitude of 20m above sea level. As shown in Table 3-1, between 1961 and 2000 the mean annual air temperature was 3.4°C and mean annual rainfall was 567 mm (Bolinder *et al.*, 2010). The site, shown in Figure 3-1, is located 2.6 km from the Ångermanälven River, in a region primarily comprised of farmland and wooded hills that are approximately 100 to 200 m high. There is less than 1% grade within a radius of 500 m of the site. Common regional farming practices generally entail growing a grass ley for 3–8 years without ploughing, followed by ploughing and growing 1–2 years of annual crops (Bolinder *et al.*, 2010). Prior to the field experiment, it is believed that the site likely grew mostly forage crops with some annual small-grains (Bolinder *et al.*, 2010).

The soil is a gleyic Cambisol that developed in silty glaciofluvial deposits (Simonsson *et al.*, 2014). The soil has an Ap horizon of 0–25 cm depth, a soil pH ~ 6 in the topsoil, and ~ 7 at 1 m depth. The soil is undrained and contains weak rust-colored mottles in the subsoil, which indicates periods of waterlogging (Jarvis *et al.*, 2017). The subsoil texture is platy and becomes massive in the layers below, which is likely as a result of annual freeze-thaw processes and traffic compaction (Jarvis *et al.*, 2017). There are few biopores in the subsoil.

Table 3-1. Geographic location and physical and climatic features for the study site in Offer, Sweden.

Lat./ Long.	Soil Type	Clay Content (%)	Silt Content (%)	Mean Annual Average Temperature	Mean Annual Average Rainfall
64.14°N 17.75°E	Silty clay loam	23 - 40	50 - 68	3.4[1]	567

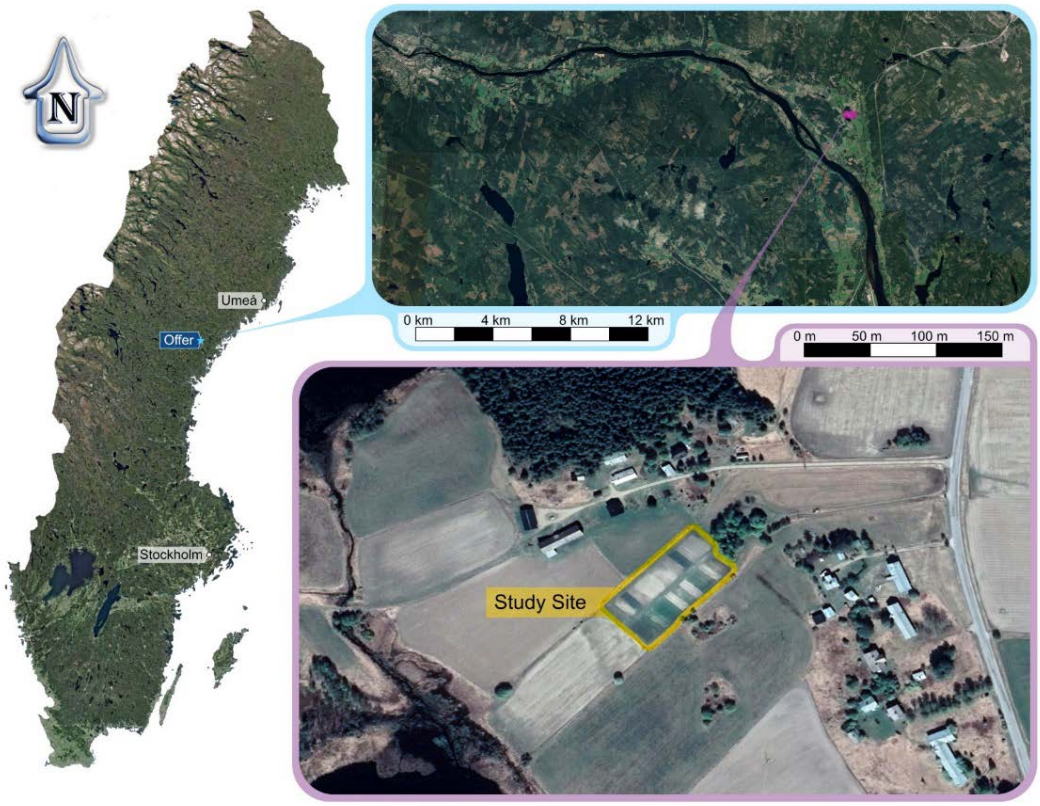

Figure 3-1. (Clockwise, starting from the left). Location of Offer within Sweden; outer lying landscape around the study site; immediate surroundings of study site, highlighted in yellow. Images captured using Google Earth Pro; first two images use compilation of satellite imagery to produce relatively cloud free images and last image was taken May 31, 2020 via CNES/Airbus.

3.2. Field experiment design

Begun in 1956, the original purpose of the experiment was to examine how varying the number of consecutive years of grass ley in combination with annual crops

[1] Precipitation and Rainfall averages calculated by Bolinder *et al.* (2010) which were based on daily climate data for the period of 1961–2000.

affects soil fertility. The experiment contains 6 randomized blocks, each of which is separated into 4 plots (20 m by 8 m in size), equaling 24 plots in total. There were four crop rotation schemes which reset every 6 years (treatments A-D) with decreasing numbers of years of grass-clover ley—A (5 yrs ley), B (3 yrs), C (2 yrs), and D (1 yr). Treatments A and B received manure twice every six years (30 Mg ha^{-1} per application), rotation C received one application (40 Mg ha^{-1}), and rotation D received no manure. The crop rotations for the four treatments can be found in Table 3-2. Each crop rotation scheme was staggered such that each stage of the cycle was present every year. Crop yields have been collected on an annual basis during the experiment, although data is missing for some years (this will be discussed in section 3.6). Additionally, SOC and BD have been monitored at various times; water retention was measured only during the first year of the study.

Previous analysis found that while treatments B-D do not display any significant differences in SOC content, they differed significantly from treatment A (D being the most different) (Bolinder *et al.*, 2010). Thus, for the purpose of this study, only treatments A and D are of interest because they exhibit the two extremes amongst the different cropping patterns and have significantly different SOC levels.

Treatment A involves 1 year of spring barley (*Hordeum vulgare L.*) with undersown ley followed by 5 years of a grass-clover ley (consisting of *Trifolium pratense L.*, *Phleum pratense L.* and *Festuca* sp.) and is plowed only after the 6^{th} year. Treatment D has one year of spring barley with undersown ley, followed by a year of grass-clover ley, and is subsequently followed by a continuous rotation of crops with plowing done every year (no tillage only between years 1 and 2). The crop rotation following the grass-clover ley initially included winter rye, followed by peas, then potatoes, and finally a root crop such as carrot or rutabaga. However, at some point—the precise year is unknown—the rotation was simplified to follow the grass-clover ley with spring barley, followed by potato, spring barley, and potato.

SOC contents for treatments A and D have been successfully simulated by Bolinder *et al.* (2012) using the ICBM model. Jarvis *et al.* (2017) measured earthworm numbers and biomass for both treatments and found that treatment A has significantly more earthworms than treatment D. Finally, soil samples have been collected in 2019 and were utilized in this study to create a new SWRC.

Table 3-2. Crop Rotations for Ongoing Offer Experiment. Treatments A-D represent different crop-rotation schemes. Treatment D1/D2 represent two different crop rotations within treatment D due to a change in the rotation (exact year unknown). Treatments A/ B received manure applications twice every six years, rotation C received one application, and rotation D received none.

Year	Treatments				
	A	B	C	D^1	D^2
1	Spring Barley (+ undersown ley)				
2	Grass-clover ley				
3	Grass-clover ley			Winter Rye	S. Barley
4	Grass-clover ley		S. Barley	Peas	Potato
5	Gr-C ley	Barley	Potato	Potato	S. Barley
6	Gr-C ley	S. Barley/ Rape/Peas		Carrot/ Rutabaga	Potato

3.3. Model description

The model utilized in this project is a carbon turnover and storage model which takes into account dynamic changes in soil pore structure and was originally presented by Meurer *et al.* (2020b). This model also draws upon the ICBM model developed by Andrén and Kätterer (1997) at SLU. Meurer *et al.* (2020b) further develop the model to account for organic matter stored in micro- and mesopores. A treatment of earthworm bioturbation is included in the model, but this is not activated in this study, since calculations showed that it has no significant impact on C storage at this site.

3.3.1. Soil organic matter storage and turnover

The ICBM model is based upon the idea that organic matter is split into fresh (*Y*) and microbially-processed (*O*) pools. Each pool has a loss (degradation) rate which follows first-order kinetics, k_y and $k_{o,}$ (year^{-1}) for the young and old organic matter, respectively. A humification (or organic matter retention) coefficient, ε (unitless), which depends upon organic matter quality and other soil factors, affects the extent of conversion from young to old organic matter. To account for differential degradation rates, a combined climate/edaphic factor, *r*, alters the k_y and k_o values. Organic matter inputs are introduced through a single variable, *I* (kg m^{-2} year^{-1}). These factors are present in the original model, which utilizes the following differential equations to describe the dynamics between pools:

$$\frac{dY}{dt} = I - k_Y r M_Y \quad (1)$$

$$\frac{dO}{dt} = \varepsilon\, k_y r M_Y - k_o r M_O \quad (2)$$

Meurer *et al.* (2020b) further developed the original differential equations by distributing fresh and microbially-processed organic matter into micro- (*mic*) and meso-pore (*mes*) regions, thereby creating four differential equations. Additional modifications have been made to the equations such that organic matter inputs are also separated into two variables, I_m and I_r, for the above-ground biomass (AGB) and below-ground biomass (BGB), respectively. The AGB inputs include litter and organic fertilizers and are assumed to contribute only to the mesopores. The BGB inputs include root and root exudates, which are assumed to be distributed proportional to micro-porosity (ϕ_{mic}) and meso-porosity (ϕ_{mes}). The separate climate/edaphic factor, r, is not utilized here; it can be assumed to be integrated into the first order rate constants. F_{prot} is introduced as a factor (between 0-1) representing physical protection in the micropore region, which reduces decomposition. This yields two differential equations that refer to the carbon pools in the mesopores and two that refer to carbon pools in the micropores:

$$\frac{dM_{Y(mes)}}{dt} = \left[I_m + \left(\frac{\phi_{mes}}{\phi_{mes}+\phi_{mic}}\right) I_r\right] - k_Y M_{Y(mes)} + T_Y \quad (3)$$

$$\frac{dM_{O(mes)}}{dt} = \left(\varepsilon\, k_Y M_{Y(mes)}\right) - \left((1-\varepsilon)\, k_O M_{O(mes)}\right) + T_O \quad (4)$$

$$\frac{dM_{Y(mic)}}{dt} = \left(\frac{\phi_{mic}}{\phi_{mes}+\phi_{mic}}\right) I_r - k_Y F_{prot} M_{Y(mic)} - T_Y \quad (5)$$

$$\frac{dM_{O(mic)}}{dt} = \left(\varepsilon\, k_Y F_{prot} M_{Y(mic)}\right) - \left((1-\varepsilon)\, k_O F_{prot} M_{O(mic)}\right) - T_O \quad (6)$$

In the above equations, T_Y and T_O are source-sink variables (kg m^{-2} year^{-1}) which account for annual mixing of young and old organic matter due to tillage and bioturbation. Annual mixing is accounted for with the factor k_{mix} (year^{-1}), wherein 1 signifies complete mixing each year and a value of zero signifies no mixing. The equations for T_Y and T_O are:

$$T_Y = k_{mix}\left(\frac{M_{Y(mic)} - M_{Y(mes)}}{2}\right) \quad (7)$$

$$T_O = k_{mix}\left(\frac{M_{O(mic)} - M_{O(mes)}}{2}\right) \quad (8)$$

This provides either positive or negative T_Y and T_O values, based on whether organic matter is gained or lost from micropores to mesopores. This gain/loss is then reflected in equations 3-6.

3.3.2. Soil physical properties

The model also accounts for the effect of SOM on porosity and pore size distribution and thus how soil layer thickness and volume change over time. The modelled soil is subdivided into five layers; each layer can change in volume (V_t) via a dynamic thickness (Δz) with a static cross-sectional area (A_{xs}). The total volume consists of the volume of pore space (V_p) and the volume of the soil solids (V_s) as follows:

$$\Delta z = \frac{V_t}{A_{xs}} \quad (9)$$

$$V_t = V_p + V_s \quad (10)$$

To account for organic matter storage, first the soil solid volume can be split into organic ($V_{s(o)}$) and mineral ($V_{s(m)}$) components. These components can be calculated from the masses of organic ($M_{s(o)}$) and mineral matter ($M_{s(m)}$) knowing the organic matter (γ_o) and mineral densities (γ_m) and the cross-sectional area (A_{xs}). The mass of organic matter will fluctuate and is the combined mass of the young and old pools in the micro- and meso-pores. The model assumes that there will be no in- or outflow of mineral material, and thus $M_{s(m)}$ is held constant throughout the model.

$$V_s = V_{s(o)} + V_{s(m)} = A_{xs}\left(\frac{M_{s(o)}}{\gamma_o} + \frac{M_{s(m)}}{\gamma_m}\right) \quad (11)$$

$$M_{s(o)} = M_{Y(mes)} + M_{O(mes)} + M_{Y(mic)} + M_{O(mic)} \quad (12)$$

The model takes into account three pore classes – macropores (V_{mac}), mesopores (V_{mes}), and micropores (V_{mic}) – of which the latter two combine to make up matrix pores (V_{mat}). The total pore volume is also divided into two pore types, structural pores ($V_{p(s)}$) and textural pores ($V_{p(t)}$). Structural pores - defined as the space between soil aggregates, which will change based on SOM inputs and the influence of chemical and physical processes - are found in all three pore classes: micropores ($V_{p(s,mic)}$), mesopores ($V_{p(s,mic)}$), and macropores (V_{mac}). The macropores are assumed to be held proportional to the total soil volume, while the structural matrix

pores vary depending on the volume of organic matter. Textural pores are defined as the space between primary soil particles. These pores will not change and consider only the matrix pores, i.e. micropores ($V_{p(t,mic)}$) and mesopores ($V_{p(t,mic)}$).

$$V_p = V_{mac} + \overbrace{V_{mic} + V_{mes}}^{V_{mat}} \quad (13)$$

$$V_p = V_{p(s)} + V_{p(t)} \quad (14)$$

$$V_{p(s)} = V_{p(s,mic)} + V_{p(s,mes)} \quad (15)$$

$$V_{p(t)} = V_{p(t,mic)} + V_{p(t,mes)} \quad (16)$$

Because a theoretical pure mineral soil with no organic matter ($M_{s(o)} = 0$) and no biological activity ($V_{p(s)} = 0$) represents the minimum value of porosity, the textural pores and mineral mass can be calculated using a minimum matrix porosity (ϕ_{min}), and a minimum thickness value (Δz_{min}).

$$V_{p(t)} = V_{p(t,mic)} + V_{p(t,mes)} = \phi_{min} \Delta z_{min} A_{xs} \quad (17)$$

$$M_{s(m)} = \Delta z_{min} \gamma_m (1 - \phi_{min}) \quad (18)$$

The distribution of textural pores can be determined using the total textural pore volume and by calculating a micropore fraction ($f_{t(mic)}$) of the matrix porosity based upon soil texture and particle size distribution as suggested by Arya and Heitman (2015).

$$V_{p(t,mic)} = V_{p(t)} f_{t(mic)} \quad (19)$$

$$V_{p(t,mes)} = V_{p(t)} \left(1 - f_{t(mic)}\right) \quad (20)$$

Boivin *et al.* (2009) demonstrated that soil properties, including soil aggregates and pore volume, varied linearly with SOC. Thus, in order to relate pore volume with SOM, an aggregation factor (f_{agg}) is introduced and can be related to organic mass, as demonstrated in equation 11.

$$V_p = V_{s(o)} f_{agg} = f_{agg} \left(A_{xs} \left(\frac{M_{s(o)}}{\gamma_o} \right) \right) \quad (21)$$

Finally, SOM, which is often measured in the field as a function of SOM (f_{som}), is defined. From this, bulk density (γ_b) - which is also measured in the field - can be defined as a function of SOM and through a substitution of equations which is explained in greater detail in Meurer *et al.* (2020b).

$$f_{som} = \frac{M_{s(o)}}{M_{s(o)}+M_{s(m)}} \quad (22)$$

$$\gamma_b = \frac{M_{s(o)}+M_{s(m)}}{V_t} = \frac{1-\phi_{mac}}{\left\{\left(\frac{f_{som}}{\gamma_o}\right)(1+f_{agg})\right\}+\left(\frac{1-f_{som}}{\gamma_m(1-\phi_{min})}\right)} \quad (23)$$

Overall porosity (ϕ) includes matrix- and macro-porosities. Macro-porosity (ϕ_{mac}), meso-porosity (ϕ_{mes}), and micro-porosity (ϕ_{mic}) can each be defined as the fraction of micro-, meso-, and macropore volumes of the entire volume. Matrix-porosity (ϕ_{mat}) can be defined by combining micro- and meso-porosities. Micro-porosity, and matrix-porosity can also be redefined based upon the SOM function and through substitution of equations, as derived in Meurer *et al.* (2020b).

$$\phi = \phi_{mat} + \phi_{mac} = (\phi_{mic} + \phi_{mes}) + \phi_{mac} \quad (24)$$

$$\phi_{mac} = \frac{V_{mac}}{V_t} \quad (25)$$

$$\phi_{mes} = \frac{V_{p(s,mes)}+V_{p(t,mes)}}{V_t} \quad (26)$$

$$\phi_{mic} = \frac{V_{p(s,mic)}+V_{p(t,mic)}}{V_t} = \frac{\left\{f_{agg}\left(\frac{M_{Y(mic)}+M_{O(mic)}}{\gamma_o}\right)\right\}+\{f_{t(mic)}\Delta z_{min}\phi_{min}\}}{\Delta z} \quad (27)$$

$$\phi_{mat} = \phi_{mic} + \phi_{mes} = \frac{\left\{\left(\frac{f_{som}}{\gamma_o}\right)f_{agg}\right\}+\left\{\left(\frac{1-f_{som}}{\gamma_m(1-\phi_{min})}\right)-\left(\frac{1-f_{som}}{\gamma_m}\right)\right\}}{\left\{\left(\frac{f_{som}}{\gamma_o}\right)(1+f_{agg})\right\}+\left(\frac{1-f_{som}}{\gamma_m(1-\phi_{min})}\right)} \quad (28)$$

It is worth noting that by calculating micro- and matrix-porosity using the redefined equations 27 and 28 and using the SOM function, meso-porosity can be calculated by subtracting micro-porosity from matrix-porosity. Additionally, because macro-porosity is a constant, by plugging the matrix- and macro-porosity values into equation 24 overall porosity can be determined.

3.3.3. Soil water retention function

In order to measure the pore size and create a dynamic system which can relate matrix potential to a SWRC, we can use the Van Genuchten (1980) (VG) equation:

$$\frac{\theta-\theta_r}{\theta_s-\theta_r} = (1 + |\alpha\psi|^n)^{-m} \quad (29)$$

where θ (m^3/m^3) is soil volumetric water content; θ_r (m^3/m^3) is residual water content; θ_s (m^3/m^3) is saturated water content (i.e. the matrix porosity, ϕ_{mat}); ψ is

soil water pressure head (cm); and α (cm^{-1}) corresponds to the inverse of the air-entry suction value. α, n, and m, are all considered to be shape parameters used to fit a WRC. m is generally considered to be the equivalent of m=1-1/n. Thus, if residual water content is considered to equal zero, the equation can be rewritten as:

$$\theta = \phi_{mat}(1 + |\alpha\psi|^{n})^{\left(\frac{1}{n}-1\right)} \quad (30)$$

Numerous studies, including Wösten et al. (2001), have shown that n is highly dependent on soil texture; in this study, soil texture is assumed to remain constant, and thus n is also held constant. If we then further rearrange the equation, α—which changes with the soil structure and pore space (Assouline & Or, 2013)—can be determined as follows:

$$\alpha = \frac{\left[\left(\frac{\phi_{mic}}{\phi_{mat}}\right)^{-\frac{n}{n-1}}-1\right]^{1/n}}{|\psi_{mic/mes}|} \quad (31)$$

in which $\psi_{mic/mes}$ is a static selected pressure head that defines the diameter of the largest micropore in soil. Per Meurer *et al.* (2020a), micropores are assumed to have a maximum pore size of 5 µm, which is the equivalent of $\psi_{mic/mes}$ = -600 cm.

3.4. Earthworm data and calculations

The project initially intended to utilize earthworm data using a bioturbation model which was originally presented in Meurer *et al.* (2020a) and has since been further developed to include soil compaction and root growth (which were not set to be utilized in this study). The intention was to utilize an annual earthworm bioturbation rate based upon an equation by Taylor *et al.* (2019) which uses laboratory-based egestion rates, biomass measurements, and an annual growth rate correction factor based on cumulative monthly soil temperatures. Taylor *et al.* (2019) found that epigeic and enecic ecotypes have a combined bioturbation rate of 0.66 g-dw-soil g^{-1}-dw-bm day^{-1} at 15°C, while endogeic ecotypes have a bioturbation rate of 1.16 g-dw-soil g^{-1}-dw-bm day^{-1} at 15°C[2].

Earthworm ecotype determination, quantification, and biomass measurements were taken in 2015 and 2016 for all four treatments and presented in Jarvis *et al.* (2017). The study found that there were no anecic adult ecotypes at the site; treatment A had a combined epigeic and endogeic ecotype dry weight (dw) biomass (bm) of 1.6

[2] Epigeic ecotypes are small litter dwellers which do not burrow, endogeic ecotypes are small topsoil dwellers found in the top 50 cm, and anecic are large deep burrowing subsoil dwellers.

g m^{-2}; and treatment D had more than five times less, 0.3 g m^{-2}. Although biomass measurements were taken of epigeic and endogeic ecotypes separately, due to the presence of unidentifiable juvenile species, an average bioturbation rate based upon the total biomass of all species was used. The resulting bioturbation rate is 0.91 g-dw-soil g^{-1}-dw-bm day^{-1} at 15°C.

Due to the lack of data available for actual monthly soil temperatures for Offer, the study utilizes a correction factor calculated for the egestion rates in Uppsala in Taylor *et al.* (2019), which was 48% of that at 15°C. However, Offer is further north and has a lower monthly mean temperature than Uppsala, so there is more snowpack in the winter, which may insulate the soil. Thus, the decision for this project was to simplify the process and utilize the Uppsala soil temperature conversion factor. The equation for annual bioturbation (Bt) includes the daily bioturbation rate at 15°C, the correction factor, conversion to a year, and the biomass.

$$Bt = 0.91 \times 0.48 \times 365\ days\ x\ bm \qquad (32)$$

Thus, the estimated annual bioturbation in plot A is 255.1 g-dw-soil m^{-2} and in plot D is 47.8 g-dw-soil m^{-2}. Despite considerable differences between plots, the bioturbation rate was still deemed to be too small to make a significant difference to the model predictions and thus bioturbation was omitted from the model.

3.5. Parameter determination

A Monte Carlo sensitivity analysis was run for the model in Meurer *et al.* (2020b), using partial rank correlation coefficients for the output variables – BD (γ_b), SOM concentration (f_{som}), and the micropore fraction (f_{mic}) – to determine which parameters strongly affected these variables, which could be determined via model calibration, and which might be correlated and thus need to be determined prior to running the model. The analysis revealed that the SOM turnover parameters – SOM retention coefficient (ε) and first-order rate coefficient for microbially-processed SOM (k_o) – significantly affected f_{som} and γ_b; γ_b was also affected by the physical soil parameters, aggregation factor (f_{agg}) and minimum porosity (ϕ_{min}). The micropore fraction of matrix porosity was strongly affected by micropore fraction of the textural pores ($f_{t(mic)}$). The sensitivity analysis determined that the physical protection factor (F_{prot}) and the mixing coefficient (k_{mix}) needs to be fixed a priori, because they are significantly negatively correlated with f_{som} and $f_{(mic)}$ respectively, the latter of which also affects f_{som} and γ_b. The sensitivity analysis additionally showed that the densities of organic matter (γ_o) and mineral matter (γ_m) are insensitive and can be fixed a priori.

Meurer *et al.* (2020b) also created a synthetic data set to further examine the model parameters and found that ε, k_o and $f_{t(mic)}$ were identifiable with calibration, while k_{mix} and F_{prot} were again unable to be identified; additionally, the first-order rate coefficient for young SOM (k_y) was also unable to be identified with calibration. The remaining parameters were not well defined and thus needed to be determined a priori. Some, including macro-porosity (ϕ_{mac}) and the aggregation factor (f_{agg}), could be calculated from field data from the Ultuna site. Others, including minimum porosity (ϕ_{min}), F_{prot}, and k_y, were taken from literature values. The mixing coefficient (k_{mix}) was highly sensitive yet unidentifiable during calibration. Meurer *et al.* (2020b) set k_{mix} to a value that worked with the model.

Because the Ultuna study contained a more comprehensive and robust dataset, certain parameters could be calibrated with model, which was not the case for Offer. Four parameters were calibrated at Ultuna: the fraction of textural micropores ($f_{t(mic)}$), the SOM retention coefficient (ε), the first-order rate coefficient for microbially-processed SOM (k_o), and organic matter input in the warm-up period ($I_{(warmup)}$), which is necessary to bring the SOC content to its initial state. At Offer, both macro-porosity (ϕ_{mac}) and the aggregation factor (f_{agg}) were initially calculated using the same method as Meurer *et al.* (2020b), although the data was too limited to produce realistic values. This also meant that $f_{t(mic)}$, k_o, and $I_{(warmup)}$ could not be calibrated in this model because they were either correlated with ε, f_{agg}, and ϕ_{mac} or there were too many free parameters to produce realistic results upon calibration; thus, these parameters also needed to be set a priori. In the end, three parameters were calibrated: ϕ_{mac}, f_{agg}, and ε. The rest – including VG's n – were set a priori. The following sub-sections explain the process of obtaining predetermined parameter values.

3.5.1. Van Genuchten parameters

In order to calculate VG's n shape parameter, water content and pressure head data from 1957 – available in Andersson (1977) – was utilized to plot a SWRC. New water content and pressure head data derived from an experiment conducted in this study was also utilized; the experiment used soil samples from treatments A and D that were collected and stored in 2019.

Using equation 30, SWRCs were produced for both datasets in Excel by plotting water content against pressure head and using a least squares error method to find a non-linear square regression to obtain VG's shape parameters n and α. The n shape parameter from each dataset was then averaged and used for this study.

The water content data from 1957 was available in 10 cm increments – starting from the surface down to 100cm depth – for pressure heads between 0.05 and 3200 m. A non-linear square regression was separately run for 0-10, 10-20, and 20-30

cm incremental depths at pressure head values of 5, 100, 300, 500, and 1000 cm. The n value was roughly the same for the two top layers (1.10 and 1.11) but was smaller at 20-30cm depth (1.04), likely attributable to a lower organic matter content. As the study focused on the top 20 cm which contained the most carbon, an average water content was calculated between 0-20cm depth, and an additional regression was run; this yielded an *n* value of 1.11 and an α value of 0.048.

An experiment was setup for the twenty-four samples collected in 2019, half of which were for treatments A and half for treatment D. The samples were collected at approximately 3-8 cm depth, in 5cm tall metal cylinders with a diameter of 7.2 cm. The samples were carefully shaved to remove excess soil and a permeable cloth was applied to the bottom of the samples. Next, the samples were saturated in water and placed in an ecotech pF suction plate module and a sequence of preset constant suction pressure values – 10, 30, 100, and 600 cm – were applied until the mass of the samples no longer varied. After each step, the samples were weighed and after the final pressure value was applied, sand with a known BD was added to the samples to fill any voids in the top of the cylinder. Finally, the samples were dried at 105°C for 68 hours to remove any remaining water and again the samples were weighed. These measurements allowed the BD, porosity, saturated water content, and water content at each pressure head value to be obtained for each sample. A detailed procedure for the experiment is shown in Table A-1 (appendix).

The samples for treatment A had noticeably more roots than treatment D. Five samples had grass growing that needed to be trimmed during the experiment; one sample in particular had grass growing in nearly every step of the lab experiment. Additionally, after saturating the samples in treatment D, the weight of the soils caused many samples to sink below the cylinder, and thus needed to be handled carefully. A number of these samples also cracked or needed to have sand added before the drying step.

Box plots were then created in matlab to examine outliers for the water contents, which can be found in the appendix (Figure A-4). The sample with grass growing in every step had significantly different BD, saturated water content, and water content values at pressure heads of -10 and -30 cm and thus the sample was not included in the calculations. A non-linear square regression was applied to the mean values for each treatment, which yielded *n* values of 1.08 for both treatments and α values of 0.545 and 0.681 for treatments A and D respectively. An average n value of 1.09, based on all three measurements, is used for this study.

After the model was run, the simulated α values were obtained for 1957, and for each treatment in 2019. These were then entered into VG's equation using the average *n* value (1.09) and plotted against SWRCs for each treatment and year, which can be found in the results.

3.5.2. Additional parameters

Many of the parameters for this study were also used in Meurer *et al.* (2020b) and were either commonly used values, or were obtained or derived from other studies. According to Skopp (2000), the particle density of mineral soils (γ_m) can range from 2.5 - 2.9 g cm^{-2}, but the particle density of quartz (2.65 g cm^{-3}) is often used; in this study, this is rounded up to 2.7 g cm^{-3}. Haan *et al.* (1994) explain that the particle density of organic matter (γ_o) can vary between 1.2 and 1.4 g cm^{-3}; this study used a density of 1.2 g cm^{-3}. Minimum matrix porosity (ϕ_{min}) occurs when mineral particles are tightly packed, and is estimated by Nimmo (2013) to be between 0.30 and 0.35 cm^3/cm^3, of which the latter value is used for this study. Given that micropores are defined as having a maximum pore size of 5 µm, Meurer *et al.* (2020b) applied a physical protection factor (F_{prot}) of 0.1, which is in accordance with observations in Kravchenko *et al.* (2015). Andrén and Kätterer (1997) used a first-order decomposition rate of fresh organic matter (k_y = 0.8 yr^{-1}) based upon previous literature; this value is also used in Meurer *et al.* (2020b) and is also applied in this study.

As discussed, a first-order decomposition rate of microbially-processed organic matter (k_o) could not be obtained via calibration for this study; thus, a value slightly smaller than the calibrated value obtained in Meurer *et al.* (2020b) was used (0.03 yr^{-1} compared to 0.036 yr^{-1}) to account for slightly colder conditions and a shorter growing season in Offer. The value is higher than the value Bolinder *et al.* (2012) use for Offer (0.007 yr^{-1}) in part because this model does not include a separate combined climate/edaphic factor; but mostly because the model includes F_{prot}, which directly acts upon k_o in the micropore region to decrease the decomposition rate by a factor of 10.

Organic matter inputs in the warm-up period ($I_{(warmup)}$), which bring the simulated SOC levels up to measured 1956 levels, were unable to be calibrated in this model. Average annual organic matter inputs for treatments A and D are 0.071 and 0.058 g cm^{-2} yr^{-1} respectively. Because the land management is similar to that of treatment B, which like treatment A received fertilizer, a value of 0.07 g cm^{-2} yr^{-1} was used for $I_{(warmup)}$. The mixing constant (k_{mix}) also took into account treatments A, D, and the land use prior to the two treatments (i.e. treatment B). A base k_{mix} value of 0.01 $year^{-1}$ was used and a multiplier was applied based upon the number of times the soil was tilled in a 6-year cycle. Treatment A was tilled once, treatment D was tilled five times, and based on treatment B, the warmup was tilled twice; this resulted in final k_{mix} values of 0.01, 0.05, and 0.02 $year^{-1}$ for treatments A, D, and the warm-up, respectively.

In order to account for textural pores in the micropore region ($f_{t(mic)}$), we use a method introduced in Arya and Heitman (2015), utilizing particle size distribution data from 1956 (Andersson, 1977) and from 2013/ 2014 (Jarvis *et al.*, 2017). The boundary pressure head between mesopores and micropores (-600 cm) and a textural porosity of 35% is used, which yields a combined estimated $f_{t(mic)}$ value of 0.93. The plot is shown in the appendix in Figure A-1.

As mentioned, to estimate ϕ_{mac} and the aggregation factor f_{agg}, a least squares regression is also conducted using equation 23 utilizing ploughed and harrowed BD and SOM data from treatments A and D 2013 and 2014 (Jarvis *et al.*, 2017) (assuming a minimum porosity of 0.3 m^3/m^3, mineral density: 2.7 g/cm^3, OM density: 1.2 g/cm^3). First the ploughed layer data was fit to get a value for the f_{agg} (4.95) and then this value was fixed to fit the harrowed layer to get ϕ_{mac} (0.05). The resulting values were, however, not utilized due to a poor fit, but the plot is shown in the appendix in Figure A-2.

The model consists of 5 layers, with a minimum (and initial) thickness of 4 cm, because most SOM was present (and measured) in the top 20 cm. A list of the parameters can be found in Table 3-3.

Table 3-3. Overview of predetermined parameters

Parameters	Fixed value
VG's shape factor, n [-]	1.09
Density of mineral matter, γ_m [g cm^{-3}]	2.7
Density of organic matter, γ_o [g cm^{-3}]	1.2
Minimum porosity, ϕ_{min} [cm^3 cm^{-3}]	0.35
Physical protection factor, F_{prot} [-]	0.1
1st order rate coefficient, k_y [$year^{-1}$]	0.80
1st order rate coefficient, k_o [$year^{-1}$]	0.03
Warmup OM inputs, $I_{(warmup)}$	0.07
Mixing coefficient, k_{mix} [$year^{-1}$]	Warm-up: 0.02 A: 0.01, D:0.05
Fraction of textural micropores, $f_{t(mic)}$	0.93
Minimum layer thickness, $\Delta z_{(min)}$ [cm]	4

3.6. Inputs for SOM data and calculations

Crop yields at Offer have been collected on an annual basis since 1957. The crops have been harvested one to three times per year. Bolinder *et al.* (2012) converted the annual crop yield data into estimated above and below ground inputs (AGB and BGB). Because the experiment is conducted in staggered periods of the rotation, crop yields for each plot within each rotation (treatments A and D) are added

together and averaged each year. Both AGB and BGB inputs were distributed uniformly among the soil layers; AGB to meso-pores, BGB to both micro- and meso-pores.

The AGB inputs are calculated and presented in Bolinder *et al.* (2012) based upon root-to-shoot ratios utilizing the crop yield data which was crop dependent. For treatment A, the fertilizer (manure) was added to AGB, which – while applied only 2 of the 6 years – was evenly distributed amongst the six-year rotation. For example, for spring Barley, 40% of the AGB production used for forage was assumed to return to the soil to account for harvest loss, foliage drop, and winter residues. BGB inputs include estimations of root biomass and 'extra-root' biomass, dependent on the crop and stage of the crop rotation. The root biomass is calculated using coefficients derived from root biomass estimations in prior studies for perennial forage and small-grain cereals; these have been calculated and discussed in more detail in Bolinder *et al.* (2012). Root biomass is included whenever a crop is harvested/removed from the rotation (not included between consecutive years of ley). The 'extra-root' biomass root component is included every year. This includes the portion of roots that die off and decompose each year (including in the winter between years of ley), cell sloughing of epidermal root tissues, and root exudates that are produced (but excludes CO_2 released by the plant) (Bolinder *et al.*, 2012; Andrén *et al.*, 1990). Bolinder *et al.* (2012) report that 'extra-root' biomass coefficients are estimated between 32-100% of the root biomass depending on the study, but recommend using an intermediate ER-C coefficient of 65% based upon a previous study presented in Bolinder *et al.* (2007).

Much of the data utilized for this study had previously been calculated and presented in Bolinder *et al.* (2012); the bulk of this data comes from the years between 1963 and 1986 which was the period with the most detailed yield data. Some additional previously unreported crop yield data was available (1987-1992 and 2001-2009) and utilized for estimating the annual SOM inputs using the same coefficients for roots and 'extra roots' that Bolinder *et al.* (2012) used. There are, however, several years in which the yield data was missing (1993-2000 and 2010-2019); for these years, an average SOM value was calculated based upon the stage of the crop rotation from the years in which data was available. The AGB and BGB inputs were converted from SOC to SOM. Per Pribyl (2010), it is estimated that SOM contains 50% C, and thus SOC was multiplied by a factor of 2. While the model uses SOM inputs, the output is converted back to SOC using the same correction factor, to match the measurements with which the data is compared with.

Figure 3-2 shows the organic matter inputs from AGB, BGB, and the cumulative annual input. Average total annual OM inputs for treatment A (with manure included) and treatment D were 0.075 and 0.0058 g OM cm^{-2} $year^{-1}$ respectively.

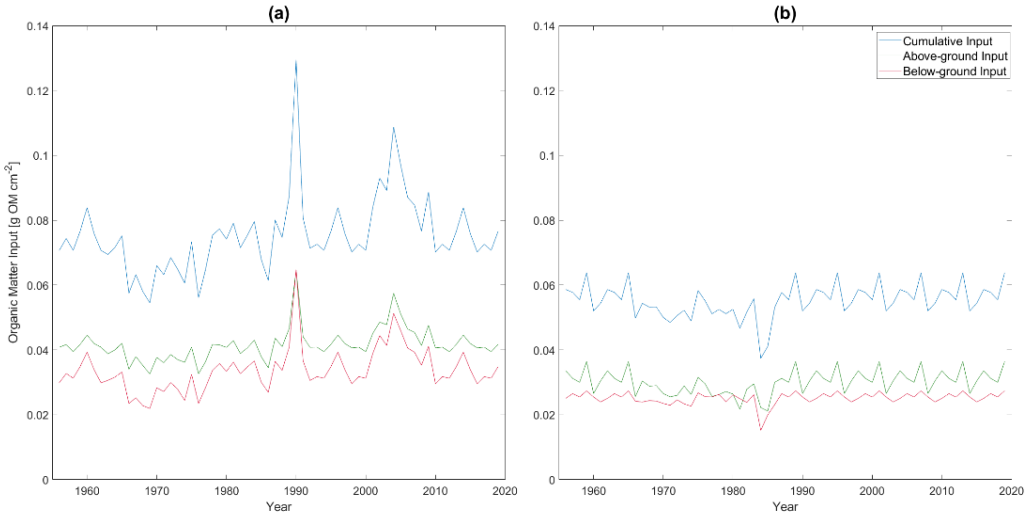

Figure 3-2. Annual organic matter inputs for (a) treatment A and (b) treatment D. Above-ground inputs, in treatment A, include a yearly OM amendment of 0.015 g OM cm^{-2}. Below ground inputs consist of root and extra-root estimates based on above ground inputs, consistent with Bolinder et al. (2012).

3.7. Additional measurements

Three measurements –SOC, BD, and micro-porosity – were taken directly from or derived using field or laboratory data; these are used as target variables for the model to try to match in order to calibrate the unknown parameters. All values are shown in Table 3-4, and sources are shown as footnotes. Standard deviations have been included when available. In 2008, Bolinder *et al.* (2012) determined SOC concentrations using dry combustion (LECO CNS 1000). SOC values were given as SOC% in literature. Micro-porosity was measured as the porosity at a pressure head of -600 from section 3.5.1. for the 1956 data and both A and D treatments for the 2019 data. BD measurements were made in 1987, 2008, and 2014; calculated using the mean value after the outliers are removed from the laboratory experiment for 2019 (a boxplot of BD can be found in the Figure A-5 in the appendix); and calculated for 1956 for 0-20 cm depth using the following:

$$BD = \frac{1-(V_P)\times 0.01}{\left(\frac{f_{som}}{\gamma_o}\right)+\left(\frac{1-f_{som}}{\gamma_m}\right)} \qquad (33)$$

Table 3-4. Variables used to calibrate model: Soil organic carbon, bulk density & micro-porosity.

Year	Rotation	SOC (kg C kg^{-1})	Bulk Density (g cm^{-3})	Micro-porosity
1956 [3]	A	0.0280	1.17	0.384
	D	0.0285	1.17	0.384
1972 [4]	A	0.027		
	D	0.023		
1987 [4]	A	0.0306	1.05	
	D	0.0204	1.25	
2008 [5]	A	0.0318 ± 0.0031	1.11 ±0.09	
	D	0.0218 ± 0.0014	1.27 ±0.06	
2010 [6]	A	0.0330		
	D	0.0215		
2014 [7]	A	0.0315 ± 0.0066	1.16 ± 0.17	
	D	1.28 ± 0.13	1.28 ± 0.13	
2019 [8]	A		1.17 ±0.11	0.356 ±0.037
	D		1.20 ±0.08	0.360 ±0.021

3.8. Model calibration

STELLA Professional software (ISEE systems) was utilized to build and run the model and simultaneously calibrate the remaining parameters against the SOC, BD, and micro-porosity measurements for treatments A and D. The model was set to use a time step of 0.25 years and included a 5000-year warm up period before imposing each treatment in order to bring the SOM pools and SOC concentrations to an initial steady-state condition. Unlike Meurer *et al.* (2020b), who set the OM warmup inputs to be introduced only in the BGB, the OM inputs were split in two so that half of the inputs were BGB and half AGB. The simultaneous calibration

[3] SOC taken directly from Andersson (1977). Micro-porosity is calculated from WRC in section 3.5.1, and BD is calculated using equation 33. Both use data from Andersson (1977)

[4] 1972 SOC and 1987 SOC and BD measurements were presented in Ericson and Mattsson (2000)

[5] SOC and BD measurements were taken from top 25 cm of soil, SOC was determined using dry combustion (Bolinder *et al.*, 2012; Bolinder *et al.*, 2010)

[6] SOC were reported in Simonsson *et al.* (2014)

[7] BD and SOC measurements were taken between 2-6 and 13-17 cm and presented in Jarvis *et al.* (2017)

[8] Soil measurements were obtained from the top 10 cm and BD/micro-porosity were calculated using lab experiment in section 3.5.1

involves running both treatments consecutively such that all parameters, unless otherwise stated, are optimized together for the warm-up period and both treatments. In the same way as for $k_{mix,}$ the OM retention coefficient is given different values for the warmup period (ε_W) and treatments A (ε_A) and D (ε_D).

The calibration uses the Powell conjugate gradient method, presented in Powell (2009), which uses an allowed range of values for each parameter (see Table 4-3) and the sum of squared errors (SSE) to try to minimize the error between the model and the three different measurement types. The calibration was run 100 times, each beginning with a different starting set of parameter values in order to ensure that the method finds the global best fit rather than a false 'local minimum' SSE.

3.8.1. Goodness of fit tests

In order to examine how well the model fits the data (SOC, BD, and micro-porosity), four statistical measures were calculated separately for each dataset: the Pearson correlation coefficient (r), root mean squared error (RMSE), mean absolute error (MAE), and the Nash-Sutcliffe model efficiency (NSE). Additionally, NSE can be extended to look at overall model efficiency (EF) by combining the datasets and using a weighted multiplier.

The Pearson correlation coefficient (r) is used to examine the strength of a linear correlation between the observed (*O*) and simulated values (*S*) by calculating the covariance and standard deviations of each (σ_o and σ_s). Values of 1 and -1 indicate a perfect positive and negative linear correlations, while 0 indicates no relationship.

$$r = \frac{covariance(O,S)}{\sigma_O \sigma_S} \qquad (34)$$

RMSE and MAE examine the average magnitude of model error (O_i - S_i). The difference between the two is that MAE weights the errors equally while RMSE gives a greater weight to larger errors. n is the number of observations in each dataset. Low values indicate less error.

$$RMSE = \sqrt{\frac{1}{n}\sum_{i=1}^{n}(O_i - S_i)^2} \qquad (35)$$

$$MAE = \frac{1}{n}\sum_{i=1}^{n}|(O_i - S_i)| \qquad (36)$$

NSE is another goodness-of-fit measure commonly used in hydrological models, which is especially useful because it is independent of units. The NSE equation, as shown in Nash and Sutcliffe (1970), is as follows:

$$NSE = 1 - \frac{\sum_{i=1}^{n}(O_i - S_i)^2}{\sum_{i=1}^{n}(O_i - \bar{O})^2} \quad (37)$$

where $\bar{O}$ is the mean observed value. A value of NSE = 1 indicates that the model perfectly matches the observed values (i.e. no model error), while negative values indicate a poor match.

NSE can be expanded upon following a method used in Larsbo and Jarvis (2005) for a solute transport model. An overall model efficiency value can be obtained for multiple data types by utilizing an adapted NSE equation to sum up the datasets by applying a weight as follows:

$$EF_{tot} = \sum_{i=1}^{m} w_i \frac{\sum_{j=1}^{n}(O_{ij} - \bar{O}_i)^2 - \sum_{j=1}^{n}(O_{ij} - S_{ij})^2}{\sum_{j=1}^{n}(O_{ij} - \bar{O}_i)^2} \quad (38)$$

$$\sum_{i=1}^{m} w_i = 1 \quad (39)$$

where n is still the number of observed values in each group; O_{ij} is the observed value; S_{ij} is the simulated value; $\bar{O}_i$ is the average observed value in each dataset; m is the number of data sets. The difference, in this case, is that a weighted value (w_i) is applied to each data set, and the NSE values are subsequently added together to get a final efficiency value (EF_{tot}). Equation 39 shows that the sum of the weights for each dataset equals one. As with NSE, an efficiency value of zero (EF_{tot} = 1) indicates a perfect match between observed and simulated values of the entire dataset, while a negative number indicates a poor match. In this study, the datatypes were initially assigned equal weights; however, due to a different number of observed values in each dataset, a weight was applied based upon the percentage of observed values in each dataset. Finally, because micro-porosity contained only two observed values, it was removed from the overall efficiency and an equal weight was applied to SOC and BD. All calculations were done in Excel or matlab.

4. Results

The model simulations of changes in young and microbially-processed SOM in mesopores and micropores for treatments A and D over the course of 63 years are shown in Figure 4-1 a and b respectively. For both treatments, SOM storage in micropores is greater than in mesopores. Additionally, the microbially-processed SOM is found at higher concentrations than fresh SOM. As mentioned previously, treatment A has higher concentrations of young SOM inputs than treatment D.

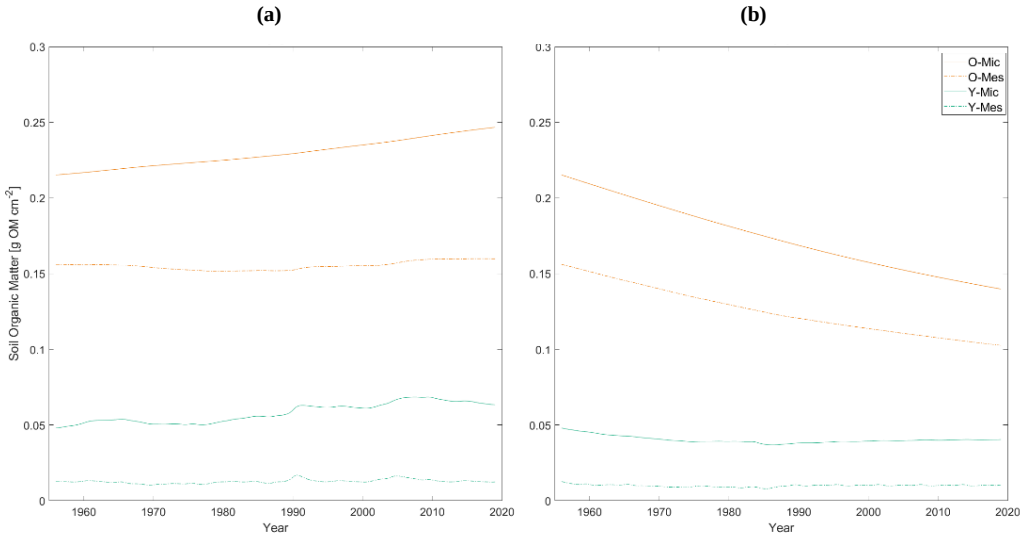

Figure 4-1. Simulated Soil Organic Matter concentrations (g OM cm^{-1}) for treatments A (a) and D (b) from 1956 to 2019. SOM is divided into micropores (mic - solid line) and mesopores (mes - dotted line) and further separated by microbially processed organic matter (O - yellow) and newly introduced organic matter (Y - green).

In treatment A, young SOM increases slightly, particularly in micropores (0.015 g OM cm^{-2}, or +32 percent). The store of microbially-processed SOM remains roughly the same in the mesopores but increases by 0.031 g OM cm^{-2} (+15 percent) in the micropores. Thus, in the end, there is an overall SOM increase of 0.050 g OM cm^{-2} (+12 percent) – both fresh and microbially-processed – in micropores.

In treatment D, the stores of both young and microbially-processed SOM remain roughly the same, with a small initial decrease of SOM in micropores before leveling off. There is, however, a significant and continuous decrease in the store

of microbially-processed SOM in both micropores and mesopores. Micropores decrease by 0.075 g OM cm^{-2} (-35 percent) and mesopores decrease by 0.053 g OM cm^{-2} (-34 percent), giving an overall decrease of 0.139 g OM cm^{-2} (-32 percent).

We begin examining how well the model simulates the data by looking at the soil organic carbon data shown in Figure 4-2. For treatment A, with 5 consecutive years of continuous ley and only one year of tillage (Figure 4-2a), we can see that the simulated SOC increases from 0.029 in 1956 to 0.032 kg C kg^{-1} in 2014, the year the final measurement was taken. This closely matches the trend in the data, with SOC increasing from 0.028 kg C kg^{-1} in 1956 to 0.031 kg C kg^{-1} in 2014. The goodness-of-fit tests are shown in Table 4-1. For treatment A, the r value is 0.91, which indicates that there is a strong correlation between the simulation and the data. The RMSE and MAE values are very small, 0.001 and 0.0009 kg kg^{-1} respectively, which further indicate that there is little overall error. Finally, the NSE value is 0.71, yet another indicator of a good model fit. It should be noted, however, that the standard deviation values that are available show a significant variation in the measurements, but given the model inputs, the simulation fits the data well.

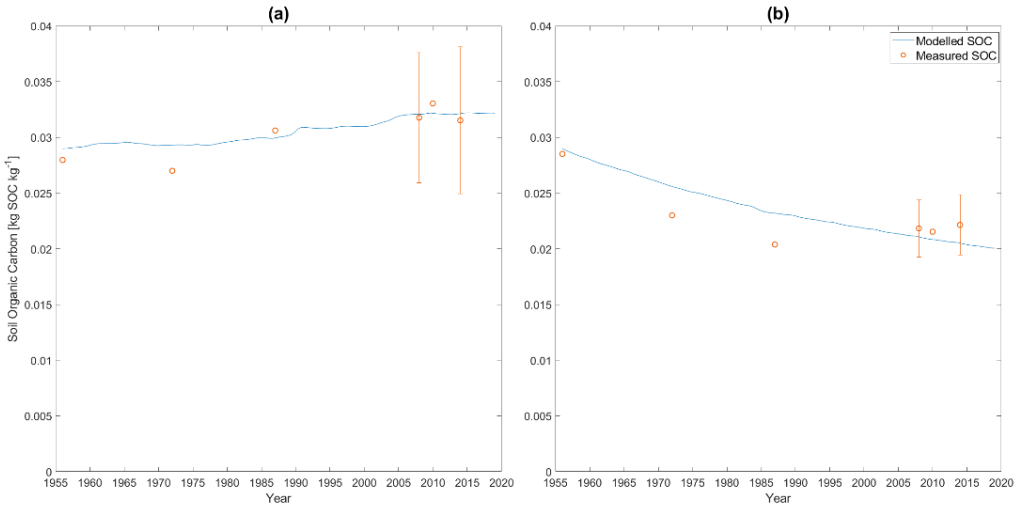

Figure 4-2. Soil Organic Carbon (kg C kg^{-1}) for treatments (a) A and (b) D. Standard deviation is shown for the measurements when available.

In treatment D, with only one year of ley and five years of arable crops, we can see in Figure 4-2b that there is a decrease in SOC in both the simulation and the measured values. The measured values initially decrease significantly between 1956 and 1987 (from 0.029 to 0.020 kg C kg^{-1}) and then increase slightly or level off in the later years to a final value of 0.022 kg C kg^{-1} in 2014. The simulated SOC does not follow this trend, but instead shows a steady overall decrease from 0.028 to 0.021 kg C kg^{-1} between 1956 and 2014. In this case, the r value is 0.83, which indicates that there is a still a reasonably strong correlation between the simulation and the data. The RMSE and MAE values are only slightly larger than treatment A, at 0.002 and 0.0015 kg kg^{-1} respectively, indicating that there is still good

agreement between the model and the data. The NSE value is 0.55, which is lower than A, but still indicates a satisfactory model performance as the value is still far above zero. This dataset has smaller standard deviation values than treatment A.

Table 4-1. Goodness of fit tests of the model and observed soil organic carbon concentration, bulk density, and micro-porosity parameters- r is the correlation coefficient, RMSE is root mean squared error, MAE is the mean absolute error, and NSE is the Nash-Sutcliffe model efficiency

	Parameter	r	RMSE	MAE	NSE
Treatment A	Soil Organic Carbon [kg C kg^{-1}]	0.91	0.001	0.0009	0.71
	Bulk density [g cm^{-3}]	-0.15	0.054	0.0414	-0.29
	Micro-porosity	-1.00	0.028	0.0280	-3.00
Treatment D	Soil Organic Carbon [kg C kg^{-1}]	0.83	0.002	0.0015	0.55
	Bulk density [g cm^{-3}]	0.66	0.041	0.0218	0.06
	Micro-porosity	1.00	0.020	0.0140	-1.72

The simulation of bulk density for treatment A (shown in Figure 4-3a) is less accurate than for SOC. The model has an r value close to zero (-0.15) and an NSE value of (-0.29). Measured BD has similar values in 1956, 2014, and 2019 (1.17, 1.16, 1.17 g cm^{-3} respectively), yet there is a strong decline in 1987 (1.05 g cm^{-3}) followed by a slight increase in 2008 (1.10 g cm^{-3}). The model, on the other hand, does not simulate the decrease in bulk density in 1972; instead the simulation shows a slight but steady decline in BD, with an initial value of 1.17 g cm^{-3} in 1956 and a final value of 1.13 g cm^{-3} in 2019. The RMSE and MAE values are 0.054 and 0.0414 g cm^{-3} respectively.

Simulations of BD in Treatment D (shown in Figure 4-3b) show smaller r and NSE values than for SOC (values of 0.66 and 0.06 respectively) indicating the model fits BD data less well, but much better than for treatment A, as NSE is still positive, indicating there is some correlation. In this case, there is a strong increase in BD measurements from the initial measurement of 1.17 g cm^{-2} in 1956 to 1.28 g cm^{-2} in 2014 before it drops back to 1.2 g cm^{-2} in 2019. The simulation shows a steady increase that emulates the increase in measured values between 1956 and 2014, with a near perfect match of simulated BD compared to the data. Yet, the RMSE and MAE values are 0.041 and 0.0218 g cm^{-3}, which indicates that there is a strong error caused by a failure to match the final measurement, as the simulated value continues to increase at the same rate. If the final BD value is removed from the statistical analysis, the r and NSE values increase to 0.99, indicating the model has a strong correlation with the other data points. Again, it should be noted that there is a large uncertainty in the final three measurements in both treatments.

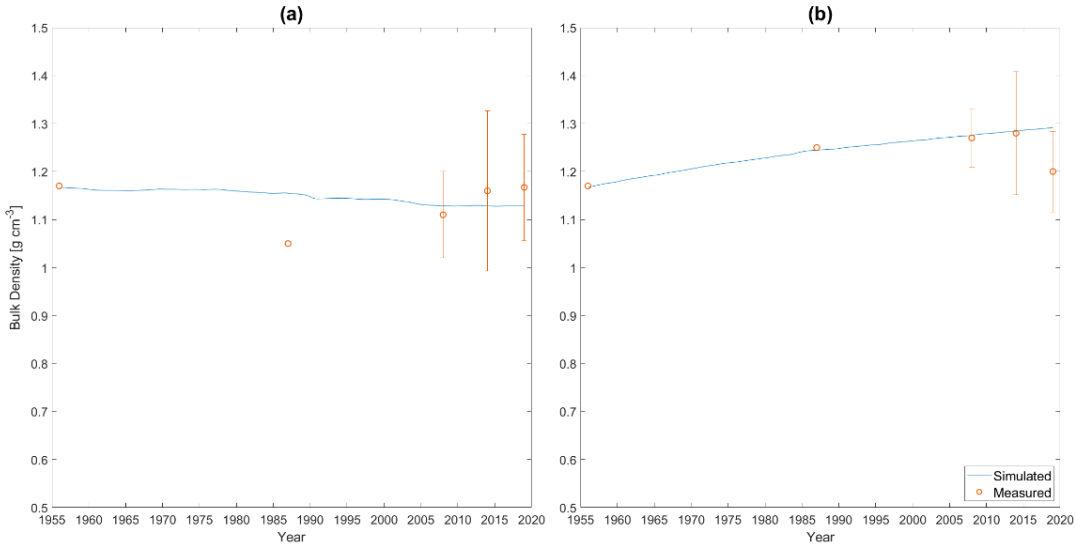

Figure 4-3. Bulk Density estimates (g cm^{-3}) were predicted by the model (blue line) to match measured data for treatments (a) A and (b) D. Error bars represent standard deviation for measurements, when available.

Only two measurements of microporosity were available (not shown) for each treatment, based on the water content at a pressure head of -600 cm from the 1956 and 2019 SWRCs. In both cases, the micro-porosity decreased slightly, dropping by 0.027 m^3 m^{-3} for treatment A and 0.024 m^3 m^{-3} for treatment D from the initial value of 0.384 m^3 m^{-3}. The simulated value had an initial value of 0.356 m^3 m^{-3} and increased in treatment A by 0.028 m^3 m^{-3} and remained relatively the same in treatment D, increasing by only 0.004 m^3 m^{-3}. Goodness-of-fit values were calculated for micro-porosity, which indicate a low correlation; but with only two data points, micro-porosity data is perhaps less reliable than SOC and BD.

An overall model efficiency (EF) was calculated for the model using an equal weight for the three parameters (0.33), a distributed weight based upon the number of samples per the entire sample pool, and an equal weight (0.5) using only bulk density and soil organic carbon. The EF value using equal weights for the three parameters was poor for both treatments, as there were negative numbers in both cases. A distributed weight led to a negative value for treatment A, but a small positive value (0.015) for treatment D, indicating a slight significance in the treatment. An EF value that considers only SOC and BD, weighting them equally, gave positive EF values for both treatments – 0.213 for treatment A and 0.308 for treatment D – which indicates the model fits both treatments reasonably well when only taking into account these two parameters.

Table 4-2. Overall efficiency (EF) values for the model using an equal weight for the three parameters (0.33), a distributed weight based upon the number of samples per the entire sample pool, and an equal weight (0.5) using only bulk density and soil organic carbon.

		Weight		
Parameter		Equal	Distributed	Equal (BD,SOC only)
Bulk density		0.33	0.39	0.5
Soil organic carbon		0.33	0.46	0.5
Micro-porosity		0.33	0.15	NA
Treat. A	EF Value	-0.849	-0.243	0.213
Treat. D	EF Value	-0.365	0.015	0.308

The model also calculates a fluctuating α value based upon equation 31 using an n value of 1.09. This value is then plugged into equation 30 to produce SWRCs for 1956 and for both treatments in 2019. Figure 4-4 shows a comparison of the simulated and initial measured soil water retention curves for each scenario. We can see that the measured values were predicted well using equation 30; however, when the fixed n value is plugged back in, using the simulated α values, it is apparent that the model does not fit the data very well. In Figure 4-4a, we see that the model is not far off from the measured 1956 values, while the 2019 simulated curves for treatments A and D (Figure 4-4b and Figure 4-4c) do not fit as well.

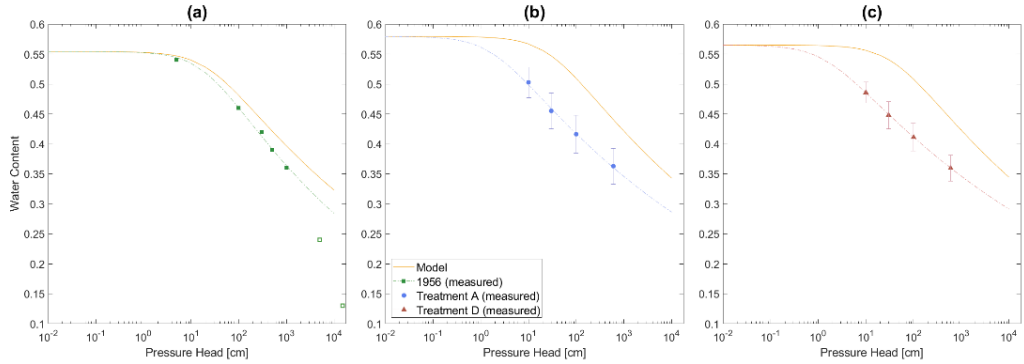

Figure 4-4. Soil water retention curves were fit to measured data (markers with standard deviation bars) for 1956 (a), and treatments A (b) and D (c) for 2019, using a non-linear square regression (dotted lines) to obtain Van Genuchten's parameters n and α. The α values obtained from the simulation were then entered into Van Genuchten's equation (assuming an averaged n value of 1.09 and the original measured/estimated saturated water content) for each year and treatment (solid line). The 1956 water content values above a pressure head of 10^3 cm (unfilled markers) were excluded from the initial non-linear square regression.

The final calibrated parameter values and confidence intervals are presented in Table 4-3. Macro-porosity has a calibrated value of 0.0336 ± 0.001 cm^3cm^{-3}, while the aggregation factor has a calibrated value of 5.03 ± 0.01. The organic matter retention coefficient (ε) for the warm-up period and treatment A had similar values, 0.276 ± 0.00 and 0.293 respectively (with a significantly higher upper limit, 0.336,

than lower limit, 0.291). The organic matter retention coefficient for treatment D had a significantly lower value at 0.145 ± 0.004.

Table 4-3. Calibrated Parameter values, with sampled range, and error margins.

Parameters	Sampled Range	Calibrated value
Warm-up OM Retention coefficient, ε_{warmup}	0.05 – 0.55	0.276 (0.276-0.276)
Treatment A OM Retention coefficient ε_A	0.05 – 0.55	0.293 (0.291-0.336)
Treatment D OM Retention coefficient ε_D	0.05 – 0.55	0.145 (0.141-0.148)
Aggregation factor, f_{agg}	2 – 6	5.03 (5.03-5.04)
Macroporosity, ϕ_{mac} [$cm^3\ cm^{-3}$]	0 – 0.3	0.0336 (0.0335-0.0336)

5. Discussion

Upon examining the effectiveness of the model, the model clearly shows an increase in SOC/SOM in treatment A compared to a loss in treatment D; we see an overall gain of 12 percent in treatment A and a loss of 32 percent in treatment D. As Figure 4-1 shows, SOM is primarily stored as microbially-processed SOM in micropores and slightly lesser amounts in mesopores. The higher first-order rate constant of fresh SOM (k_y) compared to microbially-processed SOM (k_o) clearly impacts the fresh SOM carbon pool by decomposing the fresh SOM at a much faster rate than the microbially-processed SOM. Degradation of SOM in micropores is slowed by a physical protection factor (F_{prot}). Also, the less intensive tillage represented by a smaller mixing constant (k_{mix}) and a higher SOM retention coefficient (ε) combine to decrease the loss of SOM in treatment A.

SOC was modelled with decent accuracy in both treatments, indicated by high r and NSE values. As mentioned, in treatment D the initial drop in SOC could not be modelled. Since the site had contained some crops intermixed with ley before the study, there was less of a decrease in SOC here than what is shown in other studies of previously uncultivated land (Bolinder *et al.*, 2010); however, it is likely that tillage increased in treatment D, which would destroy the soil structure and speed up decomposition of organic matter. The new land management practice could account for the stronger initial drop until SOC reached a relatively stable decline.

While the model did not manage to fit BD for treatment A, it did manage to fit the first 4 data points for treatment D nearly perfectly before the BD drop in the final year. This decrease in the measured BD value might be due to a measurement error in the laboratory experiment. As noted during the experiment, the samples for treatment D were quite weak, and during saturation sunk in the container. Such a strong decrease in BD could indicate either that soil was lost, that there were holes in the soil that could not be seen or that soil structure was destroyed via the weight of the water. It is unclear why BD initially decreased in treatment A in 1972 but subsequently increased above the initial value in the four years following; because BD is negatively correlated with organic matter, it would be reasonable that bulk density would decrease in treatment A as SOC increases, and increase in treatment D as SOC decreases. These long-term trends may have been obscured by seasonal

variations. Meurer *et al.* (2020b) noted that bulk density and macroporosity are dependent upon the time of year samples are collected and the condition of the soil.

The model went through many iterations before reaching its final parameters. As mentioned in the methods, macroporosity and the aggregation factor (f_{agg}) were originally going to be set a priori based upon two years of data but were not utilized. Because BD and SOM change over time, by setting macro-porosity and f_{agg} to match a single set of measurements the model was thrown off and thus failed to match the data from the study site. To adjust for this, macro-porosity and f_{agg} were included in the calibration, with final values of 0.03 cm^3 cm^{-3} and 5, respectively. A macro-porosity value of 0.03 cm^3 cm^{-3} is a potentially realistic value, particularly in degraded or compact soils. The f_{agg} value of 5 was high, given that in Meurer *et al.* (2020b) had a sample range of 2-4; however, in order to fit the model, f_{agg} had to be allowed to fluctuate.

The modelled soil water retention curves did not successfully match the measurements, which may be attributed to having slightly different n values, potentially due to errors in the laboratory experiment or the coarse scale in the initial 1956 experiment. Meurer *et al.* (2020b) also found that the model had difficulty in matching the measured water retention curves, potentially as a result of spatial variability and a lack of replication.

Despite various uncertainties, the model still had a positive EF value when accounting for BD and SOC with equal weights, indicating an overall satisfactory performance of the model to match BD and SOC.

5.1. Novel applications of the model

The project originally intended to explore how bioturbation affected SOM storage and turnover; however, upon calculating bioturbation, it became apparent that it would have little effect on model predictions. It is possible that sampling macrofauna populations throughout the growing period may provide clearer information on population dynamics and the effect this has on bioturbation and soil organic matter turnover.

5.1.1. Effect of SOM quality on SOM retention

Though bioturbation did not influence SOM storage, it was found that the quality of SOM is significant to SOM storage. The effect that organic matter quality has on SOM retention is well established (Kätterer *et al.*, 2011; Rasse *et al.*, 2005). Rasse *et al.* (2005) found that there was an increase in the residence time for root-

derived SOC, the extent of which was figured to be 2.4 times that of shoot-derived SOC. In a study by Kätterer *et al.* (2011) that used a humification coefficient to account for SOM retention by quality of SOM, it was found that for root-derived carbon the optimized coefficient was approximately 2.3 times higher than the same coefficient for above-ground plant residues. For this study, one SOM retention coefficient (ε) value was originally used during the calibration process for the warmup period and both treatments (A and D), which led to autocorrelation. By separating the ε values for each treatment – warmup, A, and D – we were able to model the data well, with ε values of 0.28, 0.29, and 0.15, respectively. Thus, for this study the optimized value for ε for treatment A and the warm-up is about 2 times higher than treatment D – possibly 2.4 times higher for treatment A, based on the model - for treatments that had greater amounts of root-derived carbon.

5.1.2. Effects of land-use on SOC

Multiple studies have shown that when nitrogen is readily available in soil, there is a decrease in the degradation of highly lignified material (Prescott, 2005). Roots may add lignin and suberin structures to tissues at a higher ratio than shoots, which increases the longevity of carbon storage in soil (Rasse *et al.*, 2005). Furthermore, another reason why root derived SOC has higher residence times than shoot residues is that mycorrhiza and root-hairs are able to enter into micropores, which deposits organic material in regions that are more protected from bacteria and provide anaerobic conditions that limit microbial activity (Rasse *et al.*, 2005). This could account for SOM retention values derived by Rasse *et al.* (2005) and Kätterer *et al.* (2011); data for the study by Kätterer *et al.* (2011) came from a long-term study site in Ultuna Sweden, which – like the site in Offer – was started in 1956 and examined long-term crop rotations. The study at the Ultuna site utilized a cropping system with oats grown in the first year over the whole trial, primarily spring cereals grown from 1957 to 1999, and silage maize grown from 2000 to 2009; this cropping system allowed for greater root growth due to the crop types and extended rotation periods (Kätterer *et al.*, 2011). Similarly, data from the Offer site came from cropping systems that incorporated prolonged ley periods.

At the Offer site, the warm-up period prior to the start of the study was likely mostly forage crops with some small grains, with manure supplied as fertilizer. Treatment A is also given manure and has a prolonged ley period that allows for increased root growth. Conversely, treatment D receives no manure and has only one year of ley and continual annual cropping which means there is less root growth, and thus the ε value for treatment D was half as large as those of the warmup period and treatment A. Furthermore, Ericson and Mattsson (2000) measured root depths and found that treatment A had root depths far greater than treatment D; treatment A had the most significant concentration of roots at 20 cm, and roots extended down

to 70 cm, while treatment D had no roots at 20 cm or below. Therefore, the dual-pore model accurately accounts for variation in SOM retention based on SOM quality – in this case, root-derived carbon, as supported by the findings of Kätterer et al. (2011) and Rasse et al. (2005) – which is very promising.

Considering this study in combination with previous studies at Offer (Jarvis et al., 2017; Bolinder et al., 2010; Ericson & Mattsson, 2000), as well as other long-term studies conducted in the region and abroad (Kätterer & Andrén, 1999), there is consistent evidence that a crop rotation similar to treatment A, or permanent grassland, is beneficial by increasing SOC storage and enhancing soil structure.

However, as indicated by Ericson and Mattsson (2000), while Offer saw a significant increase in SOC for treatment A, another site – Röbäcksdalen – with the same treatment saw a decrease in SOC. Ericson and Mattsson (2000) attribute this to the agricultural land use practices and field conditions that were in place prior to the start of the study. Before the experiments began, Offer likely grew mostly forage crops with some annual small-grains (Bolinder et al., 2010; Ericson & Mattsson, 2000); in contrast, Röbäcksdalen was a poorly drained grassland prior to the start of the study, and saw a decrease in SOC once it was drained (Ericson & Mattsson, 2000). Thus, it is important to consider prior land use and soil conditions when observing or modelling soil carbon dynamics. In some cases, it may be best to leave a site like Röbäcksdalen as it is, rather than convert it to grassland or another carbon-enriching crop system, as the subsequent emissions of CO_2 due to the drainage of the land may be greater than the amount of carbon that can be sequestered (Paustian et al., 1997a).

5.2. Model uncertainties

There are many uncertainties that arise when attempting to model soil organic carbon dynamics. For example, while this study assumed a SOC to SOM conversion factor of 2 based upon findings in Pribyl (2010), it is clear that SOM composition can vary considerably and – depending on the soil or sampling and measuring methods – a realistic conversion factor can range between 1.4 and 2.5. Given this, there will likely be errors when modelling SOC as inputs and conversion within the model may also vary greatly. Similarly, there are many factors that could affect the calculations of carbon inputs such as the coefficients used for biomass shoot-to-root conversion, the root and extra-root C estimates, and estimates of the above-ground residues that remain in the soil (Bolinder et al., 2012).

The model accounts for two classes of SOM, fresh and microbially processed; however, particulate organic matter will decompose faster than larger pieces of

fresh plant residue (Cole et al., 1993). Additionally, carbon may be broken down faster if the right conditions allow enzymes or microorganisms to oxidize them. Thus, both particulate organic matter and recalcitrant carbon may inherently be included in or left out of their respective SOM pools, depending upon how these inputs are determined. This could be accounted for in a more complex model by including additional factors such as nutrient composition and microbial activity.

The largest source of uncertainty is that there are so few measurements against which the model is calibrated. Several parameters had to be set 'a priori' to be able to run the model. The decomposition rates and the mixing constant could not be calibrated due to insufficient data. The macroporosity and aggregation rate could not be calculated accurately due to a small sample size (2 small datasets). The conditions prior to the experiment, considered in the warmup period, were assumed to be similar to treatment B, and as such, assumptions were made with regards to carbon inputs. Despite the lack of data, the model matched the measurements quite well, using assumptions that were generally based on literature values or calculated from the available data. More information about prior conditions, and a more detailed dataset, would have helped us calibrate or pre-calculate these parameters more accurately and would help us better understand how well the model can fit the incremental changes in the measured values.

Finally, the few data that were available often showed a high degree of variation due to a variety of sampling methods and relatively small sample sizes; it also perhaps reflects the fluctuating and complex nature of the soils, and highly localized soil response to SOM content depending on the variable conditions that exist within a plot of soil. While inputting a range of measured parameter values into the model could help explore the breadth of SOM responses to local conditions in the soil, it would be difficult to achieve, and therefore could lead to great uncertainty and leave too much room for different interpretations. Thus, in the modelling, I used the average values for these inputs, which was sufficient to examine overall trends. As more datasets and more processes are incorporated into the model, a natural range of likely outcomes for different scenarios could be generated.

5.3. Future considerations

Four years after the release of AR5, in 2018, the IPCC's "Special Report: Global Warming of 1.5°C" was published at the request of the signatories of the 2015 Paris Agreement to address the effects of anthropogenic warming on the climate. The report found that, given a 0.85°C rise in global mean surface temperature (GMST) between 1880 and 2012, an increase of 1.5 °C in GMST from pre-industrial levels will likely occur between 2030 and 2052 if warming trends continues (IPCC, 2018).

At an increase of 1.5°C, there is the risk of permanent ecosystem damage, extreme regional heat, and more frequent and severe drought periods and precipitation events (IPCC, 2018).

The likelihood of reaching a 1.5°C increase by the mid-21st century was already determined in AR5, where Representative Concentration Pathways (RCP) were developed to assess possible climate trajectories based upon future GHG concentration levels (IPCC, 2014). Of the four RCP's that were modelled and analysed, RCP 4.5 is an intermediate model, in which GHG emissions continue to rise until 2040 and then begin decreasing by 2045; this model has been widely treated as a feasible benchmark in policy-making. In 2018, it was calculated that to maintain a 1.5°C pathway like RCP 4.5 that hinges on net zero carbon emissions, it would require meeting a global annual carbon budget of between 420 $GtCO_2$ and 580 $GtCO_2$, effective immediately (IPCC, 2018). Unfortunately, in both 2018 and 2019, CO_2 emissions not only failed to be reduced enough to satisfy the global annual carbon budget, but instead increased to reach new records (Peters *et al.*, 2020). It is therefore likely that we will be unable to maintain the pathway set out by RCP 4.5, and as climate change proceeds, we can expect permafrost thaw and subsequent release of more terrestrial carbon.

If global warming leads to longer growing seasons, it will be that much more important to utilize improved land management practices such as permanent grasslands or grass ley rotations to continue mitigating CO2 emissions by limiting soil erosion, preserving soil structure, and improving SOC storage. Therefore, future SOC models should include soil pore-space structure and expand the scope of studies to account for climatic variation and examining cropping systems that can sequester carbon while providing sustenance for a growing global population.

6. Conclusion

Along with the initial study by Meurer *et al.* (2020b), this study provides further evidence that a dual-pore, dual-carbon model can successfully be utilized to model long-term SOC storage and fluxes. The model accurately represented trends in SOC contents measured in two treatments with contrasting crop rotations at a study site at Offer in northern Sweden. Simulations of changes in bulk density (BD) were less accurate for one of the treatments, but the model was accurate overall when SOC and BD were equally weighted. Additionally, despite being a more complex model, the calibrated organic matter retention coefficients for each treatment matched the findings from the studies conducted by Kätterer *et al.* (2011) and Rasse *et al.* (2005). This further supports the idea that organic matter quality, based upon extended ley treatments, increases humification and storage of SOM through the improvement of soil structure and enhanced root growth. In the future, it would be beneficial to add additional factors in the model that affect SOC storage and soil structure, such as bioturbation and root growth, as was introduced in the model by Meurer *et al.* (2020a), and explicitly accounting for microbial activity.

Finally, this study further demonstrates the importance of long-term field studies such as those done at Ultuna and Offer in Sweden, as it would not be possible to test and calibrate models without this data. Furthermore, in addition to carbon input measurements, the findings of this study indicate that BD, SOC, and water content measurements should be more regularly monitored, as these factors all influence soil structure and SOC storage capacity. It would therefore be highly beneficial to continue to fund these studies, as well as others in order to increase the availability and diversity of soil samples, SOC data, and climate data and continue improving SOC models.

Acknowledgements

I would like to begin by expressing my deepest gratitude to my advisors Katherina Meurer and Nicholas Jarvis. The culmination of knowledge that both of you have regarding soil processes and modeling has been significantly helpful during this project. Katharina, I thoroughly enjoyed working with you and appreciate your enthusiasm, knowledge, and guidance. Thank you for helping me work through and understand this tricky dataset as well as the modelling process. Nick, your ability to conceive, build, and understand such complex models, yet explain them in a simple and understandable way is inspiring. I'm grateful for your support in troubleshooting and problem solving the various issues that arose. It has been a pleasure working with both of you; I am grateful for the experience and appreciate your extreme patience throughout the thesis.

I know, however, that it takes a community to build such a complex model, and I appreciate all of the great minds and efforts that came together to complete the various iterations of the model, conduct and analyzing the field work. I would like to thank Martin Bolinder in particular, for taking the time to discuss calculations and observations from past field studies. I would also like to extend a sincere thank you to my examiner Thomas Keller and opponent Chris Wu whose thoughtful questions and valuable feedback helped refine this thesis into its final version.

Finally, I would like to thank my partner Ayesha Ali and our dog Felix, for joining me on this venture to Sweden. Ayesha, this thesis is in a much better place due to your help proofreading and discussing the thesis, as well as your constant support.

References

Andersson, S. (1977). *Studier av markprofiler i svenska åkerjordar : en faktasammanställning*. (Del II. Norrbottens, Västerbottens, Västernorrlands och Jämtlands län, 2). Uppsala: Institutionen för markvetenskap, Sveriges lantbruksuniversitet.

Andrén, O. & Kätterer, T. (1997). ICBM: THE INTRODUCTORY CARBON BALANCE MODEL FOR EXPLORATION OF SOIL CARBON BALANCES. *Ecological Applications,* 7(4), pp. 1226-1236.

Andrén, O., Lindberg, T., Boström, U., Clarholm, M., Hansson, A.-C., Johansson, G., Lagerlöf, J., Paustian, K., Persson, J., Pettersson, R., Schnürer, J., Sohlenius, B. & Wivstad, M. (1990). Organic Carbon and Nitrogen Flows. *Ecological Bulletins*(40), pp. 85-126.

Arya, L.M. & Heitman, J.L. (2015). A Non-Empirical Method for Computing Pore Radii and Soil Water Characteristics from Particle-Size Distribution. *Soil Science Society of America Journal,* 79(6), pp. 1537-1544.

Assouline, S. & Or, D. (2013). Conceptual and Parametric Representation of Soil Hydraulic Properties: A Review. *Vadose Zone Journal,* 12, p. 0.

Baker, J.M., Ochsner, T.E., Venterea, R.T. & Griffis, T.J. (2007). Tillage and soil carbon sequestration—What do we really know? *Agriculture, Ecosystems & Environment,* 118(1), pp. 1-5.

Beven, K. & Germann, P. (1982). Macropores and water flow in soils. *Water Resources Research,* 18(5), pp. 1311-1325.

Binet, F. & Curmi, P. (1992). Structural effects of Lumbricus terrestris (oligochaeta: lumbricidae) on the soil-organic matter system: Micromorphological observations and autoradiographs. *Soil Biology and Biochemistry,* 24(12), pp. 1519-1523.

Boivin, P., Schäffer, B. & Sturny, W. (2009). Quantifying the relationship between soil organic carbon and soil physical properties using shrinkage modelling. *European journal of soil science,* 60(2), pp. 265-275.

Bolinder, M.A., Janzen, H.H., Gregorich, E.G., Angers, D.A. & VandenBygaart, A.J. (2007). An approach for estimating net primary productivity and annual carbon inputs to soil for common agricultural crops in Canada. *Agriculture, Ecosystems & Environment,* 118(1), pp. 29-42.

Bolinder, M.A., Kätterer, T., Andrén, O., Ericson, L., Parent, L.E. & Kirchmann, H. (2010). Long-term soil organic carbon and nitrogen dynamics in forage-based crop rotations in Northern Sweden (63–64°N). *Agriculture, Ecosystems and Environment,* 138(3-4), pp. 335-342.

Bolinder, M.A., Katterer, T., Andren, O. & Parent, L.E. (2012). Estimating carbon inputs to soil in forage-based crop rotations and modeling the effects on soil

carbon dynamics in a Swedish long-term field experiment. *Canadian journal of plant science*, 92(6), pp. 821-833.
Bot, A. & Benites, J. (2005). *The importance of soil organic matter. Key to drought-resistant soil and sustained food and production*. (FAO Soils Bulletin, 80). Rome.
Bruand, A. & Cousin, I. (1995). Variation of textural porosity of a clay-loam soil during compaction. *European journal of soil science*, 46(3), pp. 377-385.
Childs, E.C. (1969). *An introduction to the physical basis of soil water phenomena*. London Wiley.
Cole, C.V., Flach, K., Lee, J., Sauerbeck, D. & Stewart, B. (1993). Agricultural sources and sinks of carbon. *Water, Air, and Soil Pollution*, 70(1), pp. 111-122.
Dexter, A.R. (1988). Advances in characterization of soil structure. *Soil & tillage research*, 11(3-4), pp. 199-238.
Ericson, L. & Mattsson, L. Soil and crop management impact on SOC and physical properties of soils in Northern Sweden. In: Lal, R., Kimble, J.M. & Stewart, B.A. (eds) *Proceedings of Global climate change and cold regions ecosystems*, Boca Raton, Flo2000: CRC Press, LLC, pp. pp. 123–135.
Haan, C.T., Barfield, B.J. & Hayes, J.C. (1994). 7 - Sediment Properties and Transport. In: Haan, C.T., Barfield, B.J. & Hayes, J.C. (eds) *Design Hydrology and Sedimentology for Small Catchments*. San Diego: Academic Press, pp. 204-237. Available from: http://www.sciencedirect.com/science/article/pii/B9780080571645500116.
Hsieh, Y.-P. (1992). Pool Size and Mean Age of Stable Soil Organic Carbon in Cropland. *Soil Science Society of America Journal*, 56(2), pp. 460-464.
IPCC (2014). Carbon and Other Biogeochemical Cycles. In: Intergovernmental Panel on Climate, C. (ed. *Climate Change 2013 – The Physical Science Basis: Working Group I Contribution to the Fifth Assessment Report of the Intergovernmental Panel on Climate Change*. Cambridge: Cambridge University Press, pp. 465-570.
IPCC (2018). *Global Warming of 1.5°C. An IPCC Special Report on the impacts of global warming of 1.5°C above pre-industrial levels and related global greenhouse gas emission pathways, in the context of strengthening the global response to the threat of climate change, sustainable development, and efforts to eradicate poverty*: In Press.
IPCC (2019). *Climate Change and Land: an IPCC special report on climate change, desertification, land degradation, sustainable land management, food security, and greenhouse gas fluxes in terrestrial ecosystems*: In press.
Jackson, R.B., Lajtha, K., Crow, S.E., Hugelius, G., Kramer, M.G. & Piñeiro, G. (2017). The Ecology of Soil Carbon: Pools, Vulnerabilities, and Biotic and Abiotic Controls. *Annual Review of Ecology, Evolution, and Systematics*, 48(1), pp. 419-445.
Jandl, R., Rodeghiero, M., Martinez, C., Cotrufo, M.F., Bampa, F., van Wesemael, B., Harrison, R.B., Guerrini, I.A., Richter, D.d., Rustad, L., Lorenz, K., Chabbi, A. & Miglietta, F. (2014). Current status, uncertainty and future needs in soil organic carbon monitoring. *Science of The Total Environment*, 468-469, pp. 376-383.

Jarvis, N., Forkman, J., Koestel, J., Kätterer, T., Larsbo, M. & Taylor, A. (2017). Long-term effects of grass-clover leys on the structure of a silt loam soil in a cold climate. *Agriculture, Ecosystems & Environment,* 247, p. 319.

Jarvis, N.J., Moeys, J., Hollis, J.M., Reichenberger, S., Lindahl, A.M.L. & Dubus, I.G. (2009). A Conceptual Model of Soil Susceptibility to Macropore Flow. *Vadose Zone Journal,* 8(4), pp. 902-910.

Jones, C.G., Lawton, J.H. & Shachak, M. (1997). POSITIVE AND NEGATIVE EFFECTS OF ORGANISMS AS PHYSICAL ECOSYSTEM ENGINEERS. *Ecology,* 78(7), pp. 1946-1957.

Kätterer, T. & Andrén, O. (1999). Long-term agricultural field experiments in Northern Europe: analysis of the influence of management on soil carbon stocks using the ICBM model. *Agriculture, Ecosystems & Environment,* 72(2), pp. 165-179.

Kätterer, T., Bolinder, M.A., Andrén, O., Kirchmann, H. & Menichetti, L. (2011). Roots contribute more to refractory soil organic matter than above-ground crop residues, as revealed by a long-term field experiment. *Agriculture, Ecosystems and Environment,* 141(1-2), pp. 184-192.

Keyes, S., Gillard, F., Soper, N., Mavrogordato, M., Sinclair, I. & Roose, T. (2016). Mapping soil deformation around plant roots using in vivo 4D X-ray Computed Tomography and Digital Volume Correlation. *Journal of Biomechanics,* 49.

Kleber, M. (2010). What is recalcitrant soil organic matter? *Environmental Chemistry - ENVIRON CHEM,* 7.

Kravchenko, A., Negassa, W., Guber, A. & Rivers, M. (2015). Protection of soil carbon within macro-aggregates depends on intra-aggregate pore characteristics. *Scientific Reports,* 5.

Lal, R. (2004). Soil Carbon Sequestration Impacts on Global Climate Change and Food Security. *Science (American Association for the Advancement of Science),* 304(5677), pp. 1623-1627.

Lal, R. & Follett, R. (2009). Soil Carbon Sequestration and the Greenhouse Effect.

Larsbo, M. & Jarvis, N. (2005). Simulating Solute Transport in a Structured Field Soil. *Journal of Environmental Quality - J ENVIRON QUAL,* 34.

Lepore, B.J., Morgan, C.L.S., Norman, J.M. & Molling, C.C. (2009). A Mesopore and Matrix infiltration model based on soil structure. *Geoderma,* 152(3), pp. 301-313.

Lucas, E.G., Lucas, E.G., Izquierdo, C.G., Izquierdo, C.G., Fernández, M.T.H. & Fernández, M.T.H. (2018). Changes in humic fraction characteristics and humus-enzyme complexes formation in semiarid degraded soils restored with fresh and composted urban wastes. A 5-year field experiment. *Journal of soils and sediments,* 18(4), pp. 1376-1388.

Martin, A. (1991). Short- and long-term effects of the endogeic earthworm Millsonia anomala (Omodeo) (Megascolecidae, Oligochaeta) of tropical savannas, on soil organic matter. *Biology and fertility of soils,* 11(3), pp. 234-238.

Meurer, K., Barron, J., Chenu, C., Coucheney, E., Fielding, M., Hallett, P., Herrmann, A.M., Keller, T., Koestel, J., Larsbo, M., Lewan, E., Or, D., Parsons, D., Parvin, N., Taylor, A., Vereecken, H. & Jarvis, N. (2020a). A

framework for modelling soil structure dynamics induced by biological activity. *Global Change Biology,* 26(10), pp. 5382-5403.
Meurer, K.H.E., Chenu, C., Coucheney, E., Herrmann, A.M., Keller, T., Kätterer, T., Nimblad Svensson, D. & Jarvis, N.J. (2020b). Modelling dynamic interactions between soil structure and the storage and turnover of soil organic matter. *Biogeosciences,* 17(20), pp. 5025-5042.
Nash, J.E. & Sutcliffe, J.V. (1970). River flow forecasting through conceptual models part I — A discussion of principles. *Journal of hydrology (Amsterdam),* 10(3), pp. 282-290.
Nimmo, J. (2013). Porosity and Pore Size Distribution. *Reference Module in Earth Systems and Environmental Sciences*.
Oades, J.M. (1993). The role of biology in the formation, stabilization and degradation of soil structure. *Geoderma,* 56(1), pp. 377-400.
Or, D., Leij, F.J., Snyder, V. & Ghezzehei, T.A. (2000). Stochastic model for posttillage soil pore space evolution. *Water Resources Research,* 36(7), pp. 1641-1652.
Paustian, K., Andrén, O., Janzen, H.H., Lal, R., Smith, P., Tian, G., Tiessen, H., Van Noordwijk, M. & Woomer, P.L. (1997a). Agricultural soils as a sink to mitigate CO2 emissions. *Soil Use and Management,* 13(s4), pp. 230-244.
Paustian, K., Levine, E., Post, W.M. & Ryzhova, I.M. (1997b). The use of models to integrate information and understanding of soil C at the regional scale. *Geoderma,* 79(1), pp. 227-260.
Peters, G.P., Andrew, R.M., Canadell, J.G., Friedlingstein, P., Jackson, R.B., Korsbakken, J.I., Le Quéré, C. & Peregon, A. (2020). Carbon dioxide emissions continue to grow amidst slowly emerging climate policies. *Nature Climate Change,* 10(1), pp. 3-6.
Powell, M. (2009). The BOBYQA Algorithm for Bound Constrained Optimization without Derivatives. *Technical Report, Department of Applied Mathematics and Theoretical Physics*.
Prescott, C. (2005). Decomposition and Mineralization of Nutrients from Litter and Humus. In:181), pp. 15-41.
Pribyl, D.W. (2010). A critical review of the conventional SOC to SOM conversion factor. *Geoderma,* 156(3), pp. 75-83.
Rasse, D.P., Rumpel, C. & Dignac, M.-F. (2005). Is soil carbon mostly root carbon? Mechanisms for a specific stabilisation. *Plant and soil,* 269(1), pp. 341-356.
Rawls, W.J. & Pachepsky, Y.A. (2002). Soil Consistence and Structure as Predictors of Water Retention. *Soil Science Society of America Journal,* 66(4), pp. 1115-1126.
Sanderman, J., Hengl, T. & Fiske, G.J. (2017). Soil carbon debt of 12,000 years of human land use. *Proceedings of the National Academy of Sciences of the United States of America,* 114(36), pp. 9575-9580.
Schimel, D., Braswell, B., Holland, B.A., McKeown, R., Ojima, D., Painter, T., Parton, W.J. & Townsend, A. (1994). Climatic, edaphic, and biotic controls over storage and turnover of carbon in soils. *Global biogeochemical cycles,* 8.
Schmidt, O., Clements, R.O. & Donaldson, G. (2003). Why do cereal–legume intercrops support large earthworm populations? *Applied Soil Ecology,* 22(2), pp. 181-190.

Schnitzer, M. (1991). Soil organic matter: the next 75 years. *Soil science,* 151(1), pp. 41-58.
Schnitzer, M. & Monreal, C.M. (2011). Chapter three - Quo vadis Soil Organic Matter Research?: A Biological Link to the Chemistry of Humification. In: Sparks, D.L. (ed. *Advances in Agronomy*113) Academic Press, p. i. Available from: http://www.sciencedirect.com/science/article/pii/B9780123864734000087.
Simonsson, M., Kirchmann, H., Magid, J. & Kätterer, T. (2014). Can Particulate Organic Matter Reveal Emerging Changes in Soil Organic Carbon? *Soil Science Society of America Journal,* 78(4), pp. 1279-1290.
Six, J., Bossuyt, H., Degryze, S. & Denef, K. (2004). A history of research on the link between (micro)aggregates, soil biota, and soil organic matter dynamics. *Soil & tillage research,* 79(1), pp. 7-31.
Skopp, J.M. (2000). Physical Properties of Primary Particles. In: Sumner, M.E. (ed. *Handbook of soil science*. Boca Raton, Fla: CRC Press.
Taylor, A., Lenoir, L., Vegerfors, B. & Persson, T. (2019). Ant and Earthworm Bioturbation in Cold-Temperate Ecosystems. *Ecosystems,* 22(5), pp. 981-994.
Tifafi, M., Guenet, B. & Hatté, C. (2018). Large Differences in Global and Regional Total Soil Carbon Stock Estimates Based on SoilGrids, HWSD, and NCSCD: Intercomparison and Evaluation Based on Field Data From USA, England, Wales, and France. *Global biogeochemical cycles,* 32(1), pp. 42-56.
Tisdall, J.M. & Oades, J.M. (1982). Organic matter and water-stable aggregates in soils. *Journal of soil science,* 33(2), pp. 141-163.
Van-Camp. L., Bujarrabal, B., Gentile, A.-R., Jones, R.J.A., Montanarella, L., Olazabal, C. & Selvaradjou, S.-K. (2004). *Reports of the Technical Working Groups Established under the Thematic Strategy for Soil Protection.* EUR 21319 EN/2). Luxembourg.
Van Genuchten, M. (1980). A Closed-form Equation for Predicting the Hydraulic Conductivity of Unsaturated Soils1. *Soil Science Society of America Journal*, 44.
Verdugo, P. (2012). Marine Microgels. *Annual review of marine science,* 4(1), pp. 375-400.
Watson, C.A., Atkinson, D., Gosling, P., Jackson, L.R. & Rayns, F.W. (2002). Managing soil fertility in organic farming systems. *Soil Use and Management*, 18(s1), pp. 239-247.
Wösten, H., Pachepsky, Y. & Rawls, W.J. (2001). Pedotransfer functions: bridging the gap between available basic soil data and 2.0. *J. Hydrol.*, 251, pp. 151-162.
Zhou, G., Zhou, X., He, Y., Shao, J., Hu, Z., Liu, R., Zhou, H. & Hosseinibai, S. (2017). Grazing intensity significantly affects belowground carbon and nitrogen cycling in grassland ecosystems: a meta-analysis. *Global Change Biology*, 23(3), pp. 1167-1179.
Zhou, M., Liu, C., Wang, J., Meng, Q., Yuan, Y., Ma, X., Liu, X., Zhu, Y., Ding, G., Zhang, J., Zeng, X. & Du, W. (2020). Soil aggregates stability and storage of soil organic carbon respond to cropping systems on Black Soils of Northeast China. *Scientific Reports,* 10(1), p. 265.

Appendix A

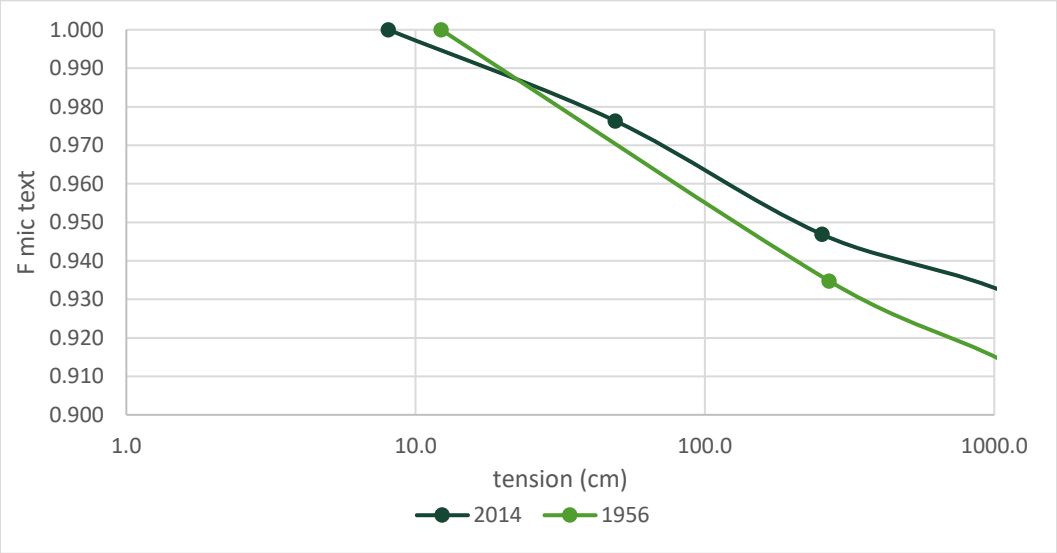

Figure A-1. Particle size distribution for 2014 and 1956 used to calculate the proportion of textural micropores are calculated as the average of both years (calculated at 600cm tension)

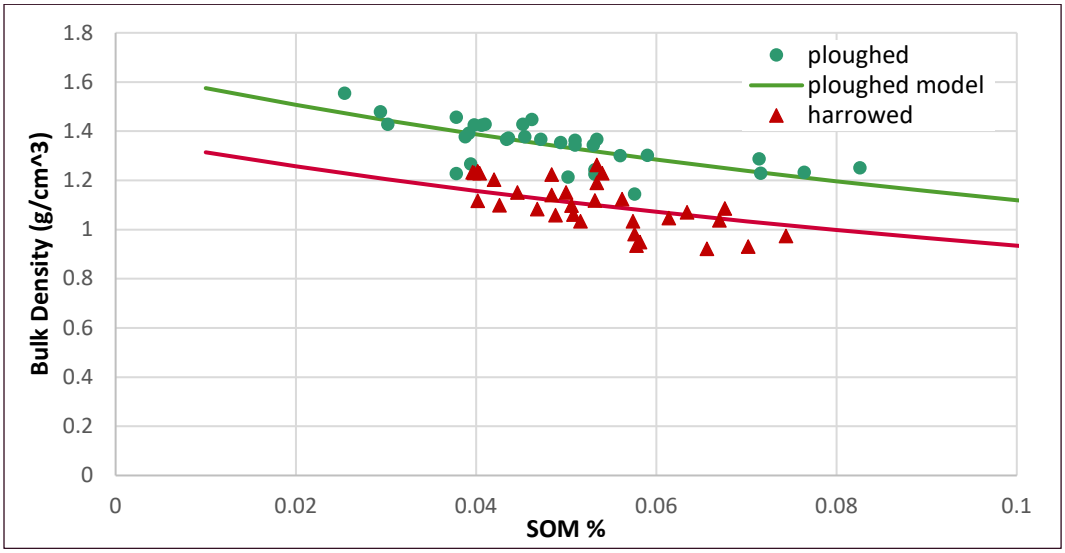

Figure A-2. Figure A-3. Model used to calculate the aggregation factor and macro-porosity using equation 23 from 2013 and 2014 data from a combined A and D treatment. The plough layer was first fit to get the aggregation factor (2.92), and then the aggregation factor was placed into the harrowed layer dataset shown in the figure, resulting in a macro-porosity value (0.216).

Table A-1. Lab Experiment Procedure conducted in order to obtain water content measurements at different suction levels for WRC used for 24 samples (12 from treatment A and 12 from treatment D) taken from Offer in 2019. (continued on next page)

Step	Task	Procedure/Notes	Included in measurements:			
			soil	cylinder	cloth/RB	sand
1 Pre-saturate Soil	A. Prep samples	Shave excess soil off top and bottom of cylinder (avoid smearing). Attach cloth/rubber band (RB) to bottom of cylinder.				
	B. Pre-saturated weight	Zero out tray and weigh sample	x	x	x	
2 Saturated Soil	A. Saturate samples	Soak samples in approximately 3 cm of water. (Originally started with less water but samples were slow to saturate, so we added more water and waited 2 days to measure)				
	B. Saturated weight	Remove samples from water and allow them to sit for approximately 2 hours (to rid excess water). Zero out tray and weigh sample (drying tray after each time)	x	x	x	
3 10 cm suction	A. Prep for 10cm suction	Place samples into PF lab station and set suction to 10 cm (+/- 1 cm)				
	B. Weight after 10cm of suction	2 days later. Zero out tray and weigh sample	x	x	x	
4 30 cm suction	A. Prep for 30cm suction	Place samples into PF lab station and set suction to 30 cm (+/- 2 cm)				
	B. Weight after 30cm of suction	5 days later. Zero out tray and weigh sample (and trim grass)	x	x	x	
5 100 cm suction	A. Prep for 100cm suction	Place samples into PF lab station and set suction to 100 cm (+/- 3 cm)				
	B. Weight after 100cm of suction	Zero out tray and weigh sample (and trim grass)	x	x	x	

7 **weight of sand and rubber band + cloth**	A. Weigh sample again with cloth/RB	Zero out tray and weigh sample again **before** removing cloth/RB	x	x	x	
	B. Weigh sample without cloth/RB	Immediately after step 7a, cloth/rubber band is removed. Final weight of sample is recorded.	x	x		
	C. Weight of sample with sand	Immediately after taking measurement in 7b, sample is kept on the scale and sand is added to sample until sand is flush to top of cylinder. Final weight is recorded.	x	x		x
	D. Weight of dry filler sand	Calculate difference between 7b and 7c				x
	E. Weight of cloth/rubber band	Zero out tray, weigh cloth/RB. (While the difference between step 7b and 7a should give the same number, I used the measurement in this step for the actual measurement as the calculated and measured weights were slightly different)			x	
8 **dry soil and weight of cylinder**	A. Place samples in oven	Place samples on small trays (6 per tray) and into oven (preset at 105°C) and leave for 48+ hours (ended up being 68 hours)				
	B. Weight of dried soil	Cool samples for approximately 30 minutes, zero out tray and weigh dried samples.	x	x		x
	C. Weight of cylinder	Scrape out soil, clean and dry cylinder, zero out tray, and weigh cylinders.		x		

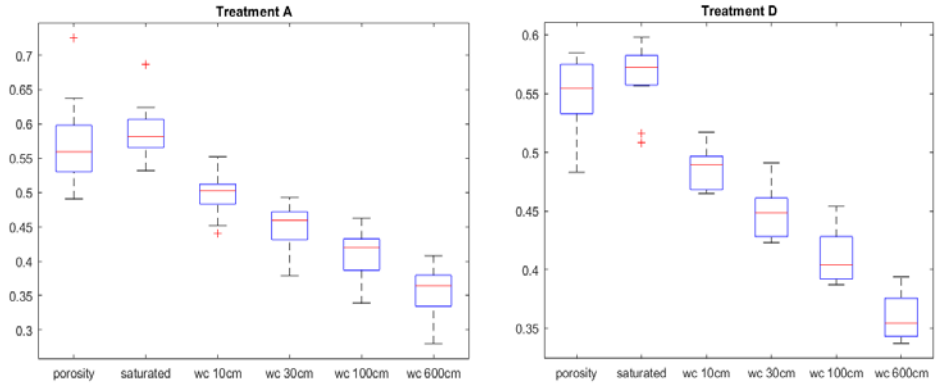

Figure A-4. Box plots for porosity, saturated water content and water content at Pf 10, 30, 100, 600 cm of treatments A and D from 2020 experiment.

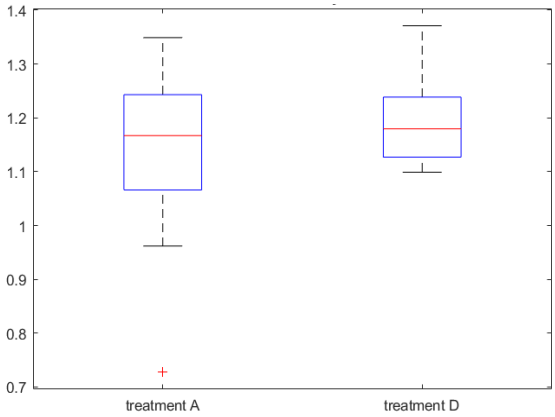

Figure A-5. Box plots for bulk density for treatments A and D calculated from 2020 experiment.